Review

OPEN

The Molecular Phenotype of Kidney Transplants: Insights From the MMDx Project

Philip F. Halloran, MD, PhD,[1] Katelynn S. Madill-Thomsen, PhD,[1] and Jeff Reeve, PhD[1]

Abstract. This review outlines the molecular disease states in kidney transplant biopsies as documented in the development of the Molecular Microscope Diagnostic System (MMDx). These states include T cell–mediated rejection (TCMR), antibody-mediated rejection (AMR), recent parenchymal injury, and irreversible atrophy-fibrosis. The MMDx project, initiated through a Genome Canada grant, is a collaboration involving many centers. MMDx uses genome-wide microarrays to measure transcript expression, interprets the results using ensembles of machine learning algorithms, and generates a report. Experimental studies in mouse models and cell lines were extensively used to annotate molecular features and interpret the biopsy results. Over time, MMDx revealed unexpected aspects of the disease states: for example, AMR is usually C4d-negative and often DSA-negative, and subtle "Minor" AMR-like states are frequent. Parenchymal injury correlates with both reduced glomerular filtration rate and increased risk of graft loss. In kidneys with rejection, injury features, not rejection activity, are the strongest predictors of graft survival. Both TCMR and AMR produce injury, but TCMR induces immediate nephron injury and accelerates atrophy-fibrosis, whereas AMR induces microcirculation and glomerular damage that slowly leads to nephron failure and atrophy-fibrosis. Plasma donor-derived cell-free DNA levels correlate strongly with AMR activity, acute kidney injury, and in a complex way with TCMR activity. Thus, the MMDx project has documented the molecular processes that underlie the clinical and histologic states in kidney transplants, and provides a diagnostic tool that can be used to calibrate biomarkers, optimize histology interpretation, and guide clinical trials.

(*Transplantation* 2024;108: 45–71).

INTRODUCTION

From the first success in identical twins in 1954, clinical kidney transplantation approaches its 70th anniversary as a work in progress.[1,2] Long-term outcomes continue to fall short of ideal. New technologies such as donor-specific antibody (DSA)[3] testing using Luminex beads, virus detection and management, blood or urine gene expression profiling, and donor-derived cell-free DNA (dd-cfDNA)[4–6] have offered incremental utility, but the field needs new understanding and ultimately new interventions to prevent and solve problems. The molecular processes at work can offer insights in this regard.

This review outlines the stepwise exploration of the genome-wide change in gene expression in kidney transplant biopsies in the Molecular Microscope Diagnostic System (MMDx) project, which aims to discover the molecular basis of the rejection and parenchymal injury states in kidney transplants. (The term parenchyma here refers to the elements of the tissue responsible for organ function, plus their supporting matrix and microvasculature, as distinct from infiltrating cells.) MMDx also aims to define the relationship between the genome-wide molecular phenotype of the transplant and other diagnostic systems such as histology, DSA, and dd-cfDNA. Some aspects

Received 26 October 2022. Revision received 7 February 2023.

Accepted 27 February 2023.

[1] *University of Alberta, Edmonton, AB, Canada.*

Clinical Trial Notation: INTERCOMEX ClinicalTrials.gov NCT01299168; Trifecta-Kidney Donor-Derived Cell-Free DNA Study ClinicalTrials.gov NCT04239703.

P.F.H., K.S.M-T., and J.R. edited and reviewed the manuscript.

P.F.H. is a full-time professor at the University of Alberta—Alberta Transplant Applied Genomics Centre (ATAGC). ATAGC has a university spinoff company, Transcriptome Sciences Inc. (TSI), to manage commercial interactions. TSI has licensed MMDx to One Lambda Inc. P.F.H. has shares in TSI, is a consultant to Natera, Inc., and has lectured for One Lambda Inc. and Natera, Inc. Neither P.F.H. nor ATAGC/TSI receive fees for biopsy interpretation. J.R. is a statistician at the University of Alberta (retired) and works part time for TSI. K.S.M-T. is a senior research scientist at TSI.

This research has been principally supported by grants from Genome Canada, Canada Foundation for Innovation, the University of Alberta Hospital Foundation, the Alberta Ministry of Advanced Education, the Mendez National Institute of Transplantation Foundation, and Industrial Research Assistance Program. Partial support was also provided by funding from a licensing agreement with the One Lambda division of Thermo Fisher. P.F.H. held a Canada Research Chair in Transplant Immunology until 2008 and currently holds the Muttart Chair in Clinical Immunology.

Supplemental digital content (SDC) is available for this article. Direct URL citations appear in the printed text, and links to the digital files are provided in the HTML text of this article on the journal's Web site (www.transplantjournal.com).

Correspondence: Philip F. Halloran, MD, PhD, Alberta Transplant Applied Genomics Centre, #250 Heritage Medical Research Centre, University of Alberta, Edmonton, AB T6G 2S2, Canada. (phallora@ualberta.ca).

ISSN: 0041-1337/20/1081-45

DOI: 10.1097/TP.0000000000004624

have previously been described,[7–11] and the technology and workflow are outlined in a recent MMDx-Heart review.[12]

The assignment of the probability that a disease is present is typically a 2-step approach: step 1, measure designated features; and step 2, interpret feature measurements using predefined algorithms. In MMDx step 1, microarrays assess messenger RNA (mRNA) expression in the biopsy, currently measuring expression of 49 495 probe sets reflecting the expression of 19 462 unique genes. MMDx step 2 interprets these measurement using ensembles of predefined machine learning–derived algorithms and compares the biopsy to a reference set of previously characterized biopsies. MMDx assesses rejection states—T cell–mediated rejection (TCMR) and antibody-mediated rejection (AMR)—and parenchymal injury states, including recent injury (acute kidney injury [AKI]), irreversible atrophy-fibrosis, and probability of survival. The extent of injury correlates with impaired function and is critical to understanding the risk of graft loss.

The timeline of MMDx development is shown in Figure 1. The reference set grows over time as new biopsies are acquired, and the diagnostic algorithms are periodically rederived. The use of a stable, fixed platform is essential to permit new biopsies to be added indefinitely to the reference set.

Table S1 (**SDC**, http://links.lww.com/TP/C772) is a list of abbreviations. **Table S2** (**SDC**, http://links.lww.com/TP/C772) lists the collaborators in the project.

BACKGROUND FOR THE MMDX PROJECT

The MMDx project arose from earlier studies of the mechanisms operating in organ transplants, particularly

FIGURE 1. Timeline of work done over the course of the MMDx-Kidney project. AMR, antibody-mediated rejection; dd-cfDNA, donor-derived cell-free DNA; DSA, donor-specific antibody; IRRAT, injury- and rejection-associated transcript; MMDx, Molecular Microscope Diagnostic System; NK, natural killer; TCMR, T cell–mediated rejection.

the role of antibodies and the regulation of gene expression. An early focus was on interactions of Fc receptors with antibodies against MHC antigens,[13,14] a theme that surprisingly re-emerged decades later with the discovery of the association of natural killer (NK) cells with AMR. Another early theme was IFNG induction of MHC and other genes in donor tissue,[15–18] acting through the donor IFNG receptor[19] and transcription factor IRF1.[20] Increased expression of IFNG-inducible genes continues to be a robust feature of all rejection.

Understanding behavior of specific genes must acknowledge complexity. For example, IFNG is highly expressed in TCMR and therefore might be considered harmful. However, in the early stages of TCMR, IFNG acting on the donor tissue protects it from early necrosis,[19–21] temporarily stabilizing the microcirculation as the inflammatory infiltrate develops. This may involve the ability of IFNG-induced donor MHC products to trigger inhibitory receptors on effector T cells: for example, donor HLAE engages effector T-cell CD94/NKG2A receptors, and donor class II can engage the effector T-cell LAG3 receptors. IFNG also plays roles in innate immunity. Expression of *IFNG*, other cytokines, and IFNG-inducible genes is also prompted by AKI,[22–24] presumably as part of the response-to-wounding. It is likely that every molecule has multiple roles in the context of the biological processes that are operating in a transplant.

The introduction of methods for studying genome-wide gene expression[25] permitted analysis of the molecular changes in TCMR in mice. The key lesion that helped to distinguish TCMR was tubulitis—the invasion of tubules by mononuclear cells, usually accompanied by interstitial inflammation, described first in native kidneys by Pollak[26] and later in rejecting transplants.[27–29] Solez et al made tubulitis a major feature of the Banff definition of TCMR.[30] Mouse kidney transplants with TCMR developed tubulitis, giving us the confidence to explore other molecular TCMR mechanisms in mice.[31] Microarray studies in mouse kidney transplants revealed that TCMR induced massive changes in gene expression, reflecting IFNG effects, infiltration, and activation of effector T cells and myeloid cells,[32,33] and parenchymal injury and dedifferentiation. In rejecting kidneys, IFNG induces increased expression of many genes involved in antigen presentation such as MHC class I and class II, proteosomes PSMB8 and PSMB9, invariant chain CD74, and beta2 microglobulin, and other genes such as guanylate binding proteins, IDO1, WARS, and the IFNG-inducible chemokines CXCL9, CXCL10, and CXCL11. In rejecting kidney transplants in IFNG knockout mice, the increase in expression of the IFNG-inducible genes was reduced but not eliminated,[21,22] presumably because other cytokines participate in the induction of these genes, often synergistically with IFNG (eg, TNF). Hence, we call these genes "IFNG-inducible," not "IFNG-induced."

The absence of tubulitis in AMR was key to distinguishing AMR from TCMR. Mouse kidney transplant models do not spontaneously manifest a state that resembles human AMR, probably because mouse NK cells are different from human NK cells[34,35] (see below). Thus, AMR had to be defined by observing human kidney transplants, where it emerged as a microcirculation process that lacked tubulitis and was associated with DSA.[36] As recently reviewed,[37] the discovery by Feucht et al of C4d staining of the microcirculation in AMR[38,39] was critical to the acceptance of AMR in Banff guidelines.[40] Ironically, despite the importance of DSA and C4d in the initial recognition of AMR, we eventually found that C4d staining[41] and even circulating DSA[42] were often negative in AMR.

Pathogenesis-based Transcript Sets

Genes usually change their expression in tissues not as individual genes but in coordinate patterns. We used experimental models, cell lines, and biopsies to annotate thousands of genes as members of pathogenesis-based transcript sets (PBT) (https://www.ualberta.ca/medicine/institutes-centres-groups/atagc/research/gene-lists.html). Some commonly used PBTs are listed in Table 1, include quantitative cytotoxic T cell-associated transcripts[52]; IFNG- and rejection inducible transcripts (GRITs)[32]; injury- and rejection-associated transcripts (IRRATs)[48]; alternative macrophage activation transcripts (AMATs)[53]; and quantitative constitutive macrophage associated transcripts (QCMATs).[54] We mapped the transcripts characteristic of human effector T lymphocytes and NK cells in vitro and in kidney biopsies.[43,55] To monitor parenchymal dedifferentiation, we annotated kidney transcripts (KT) highly expressed in normal kidney that are reduced in expression after TCMR or injury.[56,57]

THE GENOME CANADA MMDX PROJECT: DEFINING REJECTION AND INJURY IN TRANSPLANT BIOPSIES

Approaching the Analysis of Biopsies

The explosion of knowledge and technology that followed the sequencing of the human genome set the stage for our Genome Canada-funded project, a large-scale peer-reviewed grant to explore human organ transplant biopsies using genome-wide microarrays to understand the mechanisms operating in clinical states and to develop new dimensions in diagnostics. The strategy was to measure mRNA expression in intact RNA (from biopsies stabilized in RNA*later*), avoiding formalin-paraffin fixation because this damages the mRNA. We develop machine-learning algorithms for the interpretation of the mRNA

TABLE 1.

Commonly used PBT sets[a]

Transcript set	Abbreviation	Description of the transcripts
TCMR-related	QCAT	Cytotoxic T cell associated[43]
AMR-related	DSAST	DSA selective[44]
	NKB	NK cell transcript burden[45]
	AMR-RAT[b]	AMR selective[46]
	GRIT	Interferon gamma-inducible[47]
Increased after recent injury	IRRAT30	Injury-repair response associated[48]
	FICOL	Fibrillar collagen transcripts[49]
	IRITD3	Injury-repair induced transcripts, day 3[50]
	IRITD5	Injury-repair induced transcripts, day 5[50]
Atrophy-fibrosis	IGT	Immunoglobulin transcripts[51]

[a] https://www.ualberta.ca/medicine/institutes-centres-groups/atagc/research/gene-lists.
[b] The abbreviation AMR is used by journal convention but official abbreviations used in the MMDx papers and website is usually "ABMR."
AMR, antibody-mediated rejection; DSA, donor-specific antibody; DSAT, DSA-selective transcripts; FICOL, fibrillar collagen; GRIT, IFNG-inducible transcripts; IGT, immunoglobulin transcripts; IRITD3, injury-repair induced, day 3; IRITD5, injury-repair induced, day 5; IRRAT, injury- and rejection-associated transcript; NKB, NK cell burden; PBT, pathogenesis-based transcript; QCAT, cytotoxic CD8 T cell-associated transcript; TCMR, T cell–mediated rejection.

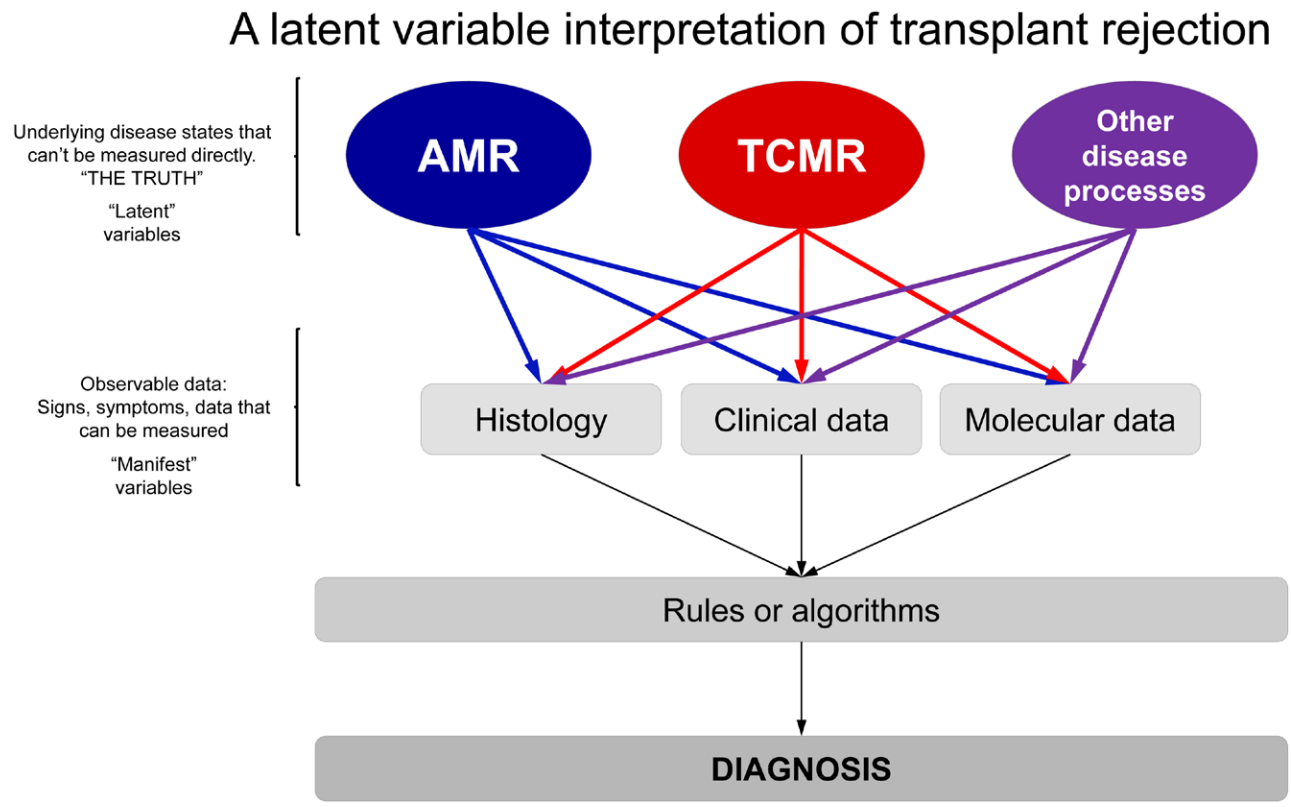

FIGURE 2. Latent variable interpretation of transplant rejection. True disease states are "latent variables" that can seldom be known with absolute certainty. Observable measurements ("manifestations": histologic, clinical, and molecular data) of the underlying diseases are used to assign a diagnosis. The Banff system uses histologic lesions + DSA + C4d (step 1) to make diagnoses using consensus rules/expert opinion (step 2). MMDx measures gene expression (step 1) to assign disease states/probabilities (step 2) using: (A) scores from supervised methods—classifiers based on correlations/associations between gene expression and histologic diagnoses/lesion scores, and (B) unsupervised methods combining scores from (A) and gene set (PBT) scores. Once in place, both Banff and MMDx require only 1 type of data to assign diagnoses in new samples—histology/DSA for Banff, and gene expression for MMDx. AMR, antibody-mediated rejection; DSA, donor-specific antibody; MMDx, Molecular Microscope Diagnostic System; PBT, pathogenesis-based transcript; TCMR, T cell–mediated rejection.

measurements in rejection and injury; accumulate a reference set of well-characterized biopsies against which new biopsies could be compared using locked, predefined algorithms; and retain the biopsy mRNA as a resource. We focused on indication biopsies because they include all phenotypes, including those found in protocol biopsies.[58] The technology is detailed in a previous review.[12]

The MMDx project approaches the disease states as latent variables—unknowable truths that can only ever be estimated by various approaches (Figure 2). We consider the phenotype labels assigned by clinical experience and histology as guides to the discovery of the underlying truth (the real disease). Accordingly, we use our molecular system not only for making diagnostic evaluations in new biopsies but also for reinterpreting the previous biopsies in the development set. We believe that while molecular variables are more highly correlated with the disease state than the standard-of-care histologic or clinical data,[59] there is also important information in the histologic or clinical variables to assist the development of the molecular classifiers. As such, some MMDx algorithms are trained on the molecules correlating with histologic lesion scores and clinical measurements such as estimated glomerular filtration rate (eGFR), proteinuria, or DSA.

The steps in classifier development are shown in Figure 3, and the main classifiers are listed in Table 2. When publishing classifier results, we always present the *test set* scores for biopsies—those obtained in the left-out portion of the cross-validation process—and not the training set results. The final classifier (trained on the entire development set) is then locked for use in new biopsies, minimizing overfitting.

Discovery of the truth about disease states is never finished. For example, many "truths" we believed when we helped initiate the Banff guidelines in 1991 have now been disproven. Diagnostic systems are estimates of the unknown truth—we accumulate evidence and formulate an interpretation but "the truth is out there…"

Estimates of the true disease phenotype vary by their step 1 input (the disease features assessed) and the step 2 algorithms (the way these features are used to come to a diagnosis). There are many estimates of the disease state – clinical observations, histologic and molecular biopsy interpretation, dd-cfDNA, DSA—that the clinician integrates in making a management decision. Some estimates come closer to the truth than others, some phenotypes are simpler to assess, and all such estimates remain subject to future reinterpretation. Data-driven approaches to the truth, like MMDx, present an advantage because the continued evolution is informed solely by unbiased and reproducible data that can used to correct errors.

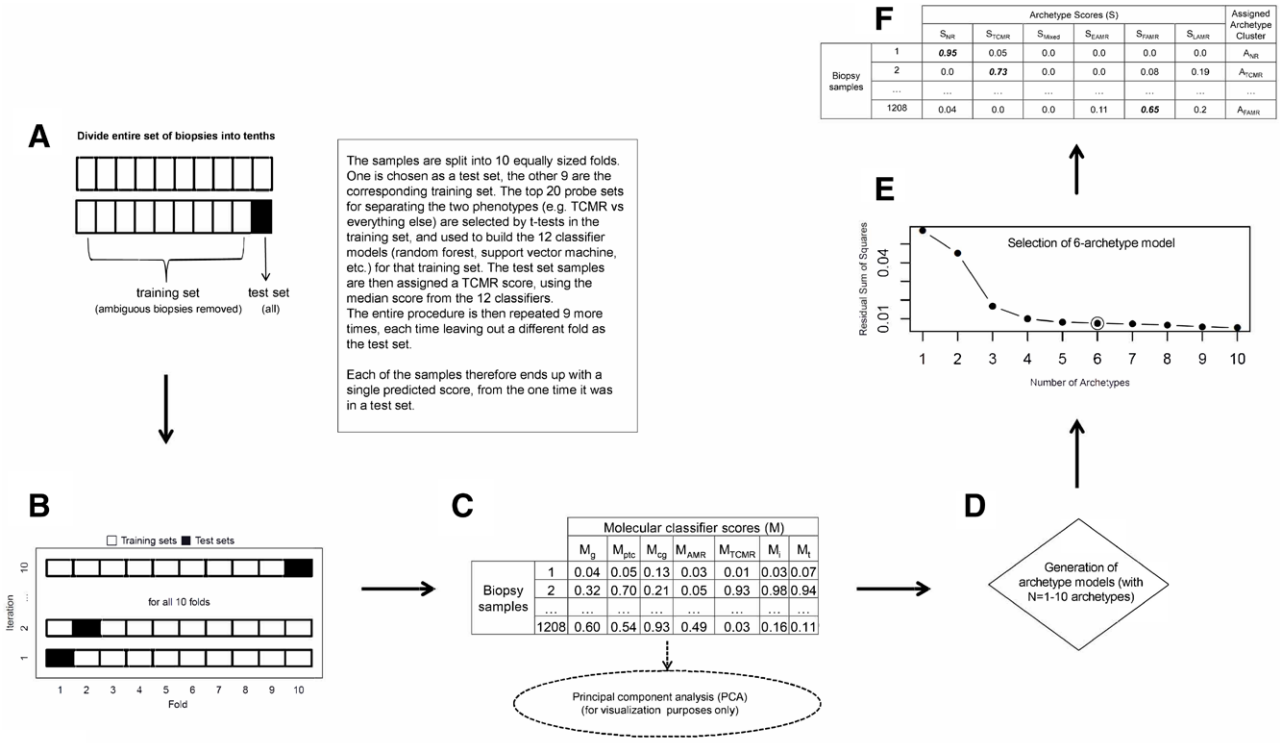

FIGURE 3. Classifier algorithm flowchart.[60] A, Ten-fold cross-validation is illustrated, with each of the 10 folds shown as they are used in both the training and test sets. B and C, How the base classifiers (TCMR, AMR, i > 1, t > 1, g > 0, cg > 0, ptc > 0) were developed. For each of the 7 base classifiers: (B) 10-fold cross-validation is performed, randomly splitting the 1208 biopsies into 10 folds of equal or near-equal size. For each of 10 iterations, 1 fold is left out as a test set (black box), and a classifier is developed using the remaining 9 folds (white boxes) as the training set. All aspects of classifier development, including probe set selection, are carried out from scratch within the training set samples at each iteration. The top 20 (by *P* value) differentially expressed probe sets comparing the binary phenotypes within the training set are selected as input features for the classifier. Twelve different classifier algorithms are developed in each training set, generating 12 scores for each test set sample (1 for each classifier algorithm). The median of these 12 is used as each test set sample's final score. This process is repeated over all 10 iterations, resulting in each biopsy being in a test set once and receiving a single value. C, This is repeated for each of the 7 base classifiers, resulting in a 1208 × 7 matrix of classifier test set scores. D–F, The archetypal analysis. These data are used as the input for both the principal component analysis (used for visualizing the multivariate distribution) and the archetypal analysis. D, We generated 10 archetype models (with n = 1–10 archetypes). The residual sum of squares decreases with increasing numbers of archetypes (scree plot in E). We selected 6 archetypes (circled point in E) as the final archetypal model. F, All biopsy samples are assigned a score for each of the 6 archetypes, and cluster assignments are made based on the highest score within that biopsy. The tables included show what typical data look like but do not represent actual results. AMR, antibody-mediated rejection; cg, transplant glomerulopathy; EAMR, early-stage AMR; FAMR, fully developed AMR; g, glomerulitis; i, interstitial inflammation; LAMR, late-stage AMR; M, molecular classifier scores; NR, no rejection; ptc, peritubular capillaritis; S, archetype score; t, tubulitis; TCMR, T cell–mediated rejection.

Relating Gene Expression to Disease Phenotype

MMDx step 1 is the measurement of gene expression in a set of biopsies, for example, 1208 biopsies used in the current report, analyzed as a matrix with 1208 columns (biopsies) and 49 495 rows (probe sets). This is high dimensionality data—many samples, each with thousands of measurements. Analysis requires rigorous approaches to avoid pitfalls.[9,67,68]

We can define alterations in gene expression as the following:

1. Disease-*associated*, determined by comparing the disease to "normal" tissue. In diagnostics, such analyses have "limited challenge bias": changes between a disease state and normal tissue are of less value than the changes that distinguish the disease state from other diseases as well as from normal tissue.
2. Disease-*selective*, determined by comparing the disease to "everything else," for example, all other biopsies in the reference set, including normal and all diseases and forms of injury. For example, TCMR has increased expression of TCMR-selective transcripts reflecting T cell activation (eg, *LAG3*) but also of transcripts reflecting parenchymal injury that are increased in many types of nephron damage.

It is important to note that no single transcript is 100% selective for any form of rejection. This is the main rationale for combining the expression of many genes rather than relying on one. Averaging the standardized expression of a collection of relevant genes—a transcript set—can improve diagnostic accuracy—in effect taking an unweighted average of the expression of the genes. We use machine learning techniques to maximize the information content of the genes, rather than simply averaging them.

We interpret the cell type most responsible for expressing a particular gene based on the literature, sources such as the Human Protein Atlas,[69] and expression in our cell panel in vitro. However, we acknowledge that we never know exactly what cell in a biopsy expresses that gene. Single-cell RNA sequencing and 3-dimensional transcript analyses have great potential for eventually designating the expression of each gene in various cell types.[70,71]

TABLE 2.

Main kidney classifiers developed during the MMDx-Kidney project

Rejection or injury	Category	Name	Description—trained on and predicting:
Rejection-related classifiers	TCMR-related	i-score ($i>1_{Prob}$)	probability of histologic i-lesion score > 1[61]
		t-score ($t>1_{Prob}$)	probability of histologic t-lesion score > 1[61]
		TCMR ($TCMR_{Prob}$)	probability of histologic TCMR diagnosis[60]
	AMR-related	AMR (AMR_{Prob})[a]	probability of histologic AMR diagnosis[62]
		Glomerular double contours ($cg>0_{Prob}$)	probability of histologic cg-lesion score > 0[61]
		Peritubular capillaritis ($ptc>0_{Prob}$)	probability of histologic ptc-lesion score > 0.
		Glomerulitis ($g>0_{Prob}$)	probability of histologic g-lesion score > 0[61]
		DSA_{Prob}	probability that biopsies with be from DSA-positive patients[63]
	All rejection-related	Rejection (Rej_{Prob})	probability of any histologic diagnosis of rejection[64]
Injury-related classifiers	Recent injury-related	$lowGFR_{Prob}$	probability of GFR ≤30[65]
	Atrophy-fibrosis	ci-score ($ci>1_{Prob}$)	probability of histologic ci-lesion score > 1[66]

[a] The abbreviation AMR is used by journal convention but official abbreviations used in the MMDx papers and website is usually "ABMR."
AMR, antibody-mediated rejection; cg, transplant glomerulopathy; DSA, donor-specific antibody; g, glomerulitis; GFR, glomerular filtration rate; i, interstitial inflammation; ptc, peritubular capillaritis; t, tubularitis; TCMR, T cell–mediated rejection.

General Issues in Biopsy Assessment

MMDx is subject to limitations that affect all biopsy assessments[12,59]:

1. Anatomical variation within the organ, for example, medulla versus cortex;
2. Patchiness of the disease process within the organ, for example, intense focal infiltrates;
3. Boundary cases near the cutoff defining the positive versus negative condition;
4. The ability of small tissue samples to represent the organ. Because MMDx has been developed in IRB-approved protocols, the amount of tissue has been constrained to about a 3-mm segment of a core. The *ideal* amount of tissue must continue to be evaluated (see below).

In terms of anatomical variation, MMDx estimates the percent cortex in a kidney biopsy by measuring the expression of podocin (*NPHS2*). MMDx can detect rejection and injury in medulla, with the caveat[72] that biopsies that are mainly medulla often distort some scores, for example, late-stage AMR and the transplant glomerulopathy (cg)-classifier.

Although results can be affected by technical processing details,[73] MMDx processes are highly standardized, and using RNA*later* to stabilize biopsies guarantees that MMDx can read virtually every biopsy submitted.[72]

Measures of the molecular rejection and injury changes in transplanted tissue tend to be continuous, not dichotomous or categorical, but diagnostic systems must divide them into positive versus negative at a boundary because the clinician must make treatment decisions. Biopsies that fall near boundaries are difficult to classify in a binary fashion. However, having defined the boundary, molecular studies can study subtle changes below diagnostic boundaries, that is, "what lies beneath."[63,74]

Steps in Assessing Biopsies

MMDx step 1 transcript measurements are precise (>99% reproducible)[75] on the piece of tissue provided, therefore the step 2 classifier and archetype scores derived mathematically from those measurements are also precise. To optimize our assessments, step 2 uses ensembles of classifiers, each derived using a different machine learning algorithm. *Ensembles of independent estimates are more likely to be accurate than single estimates*. Each classifier on the MMDx report is actually the median of an ensemble of 12 different machine learning classifier scores for that biopsy.[59] The combination of the 3 different AMR ensemble classifiers and 2 different TCMR ensemble classifiers on the MMDx report adds another level to the ensemble approach. Alternative classifiers have subtle differences in their training algorithms, for example, whether samples with mixed rejection can be included in the positive class or excluded.

Histologic biopsy assessment usually involves assessment of lesions, DSA, and C4d in step 1, and interpretation by guidelines step 2,[76] and has limitations in reproducibility.[60] Variability can be reduced by having an "ensemble" of observers *independently* read the biopsy[77] and using some form of averaging, but this is not the usual practice and is not specified in the Banff guidelines.

In disease states, genes change expression in large coordinate groups, not as individuals. As we sequentially mapped the rejection- and injury-related elements operating in biopsies, we discovered that the changes reflected groups of genes that share behaviors in the biopsies—PBTs—indicating "herd movements."[78] These reflected biological mechanisms affecting many genes simultaneously, either reflecting change in expression in the tissue, a change in the cell population, or both.

For example, when we aligned all biopsies by their ascending scores for expression of cytotoxic T cell-associated transcripts, many other gene sets showed similar alignment, for example, increased IFNG effects (GRIT) and dedifferentiation—decreased expression of normal kidney transcripts (KT1, Figure 4). Similar coordinate changes in gene set expression were observed in different disease states, with no absolute separation. Because disease states vary in stage, intensity, and treatment effects, molecular features present a continuous spectrum rather than dichotomous groups. This is particularly relevant for organ transplants, where rejection is superimposed on the effects of injury from the donation-implantation process and donor aging.

As a member of a "herd," an individual transcript can provide diagnostic information that represents the entire biologic process, correlating with altered expression of

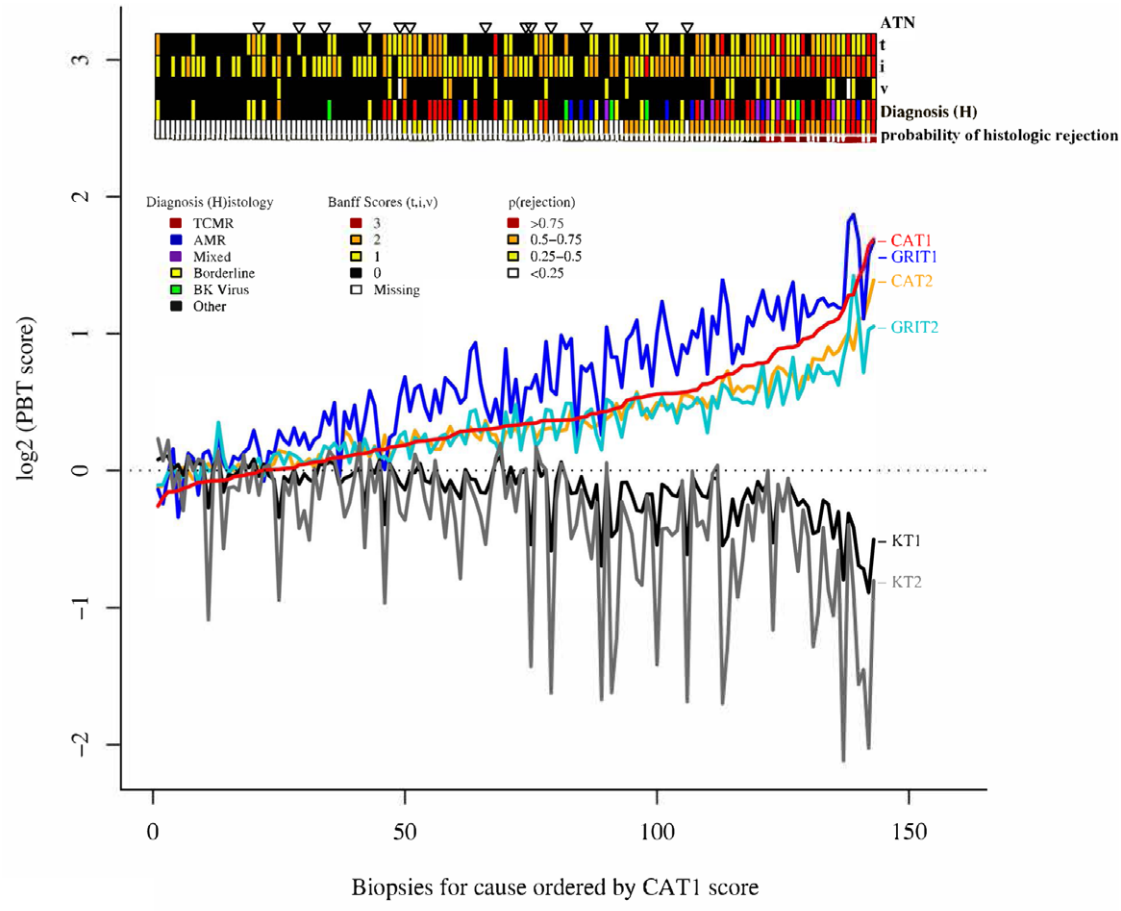

FIGURE 4. Relationship between PBT scores, histopathologic lesions, histologic diagnosis, and classifier predictions.[78] Biopsies for cause (N = 143) were sorted based on the CAT1 score (from lowest to highest). According to this order, scores for all PBTs (CAT1, CAT2, GRIT1, GRIT2, KT1, and KT2) are illustrated for each individual biopsy for cause. The panel above the graph illustrates the relationship of the PBT scores to the histologic diagnosis of ATN, the interstitial infiltrate (i score), tubulitis (t score), intimal arteritis (v score), and the probability of rejection (%) predicted from a classifier. Biopsies were sorted based on the CAT1 score, and the relationship between PBT scores, diagnosis, and classifier predictions are shown. ATN, acute tubular necrosis; CAT, cytotoxic T lymphocyte-associated transcripts; GRIT, IFNG-inducible transcripts; i, interstitial infiltrate; KT, kidney transcripts; PBT, pathogenesis-based transcript set; t, tubulitis; v, intimal arteritis.

large numbers of other transcripts. For example, increases in LAG3 will be associated with increases in many related genes in activated T cells. At a false discovery rate of 0.05, there are often thousands of genes in these herds.

There is no unique "signature" for a disease process. Most genes will be used in many processes, and the top-ranked transcripts will vary with the test applied and the composition of the population being tested.

Mapping Elements of Molecular Rejection

All Rejection Transcripts

In 703 biopsies, we defined transcripts shared by TCMR and AMR[11,47,64] versus everything else. Across all biopsies, rejection is characterized by IFNG-inducible transcripts genes such as CXCL11, WARS,[64] IDO1, and GBP4, and by transcripts shared by effector T cells and NK cells such as KLRD1 and CCL4 (Figure 5A).[11,47]

For analytical purposes, we also assembled a set of 600 rejection-associated transcripts by combining the top 200 probe sets selective for each state: TCMR, AMR, and all rejection.[47] Eliminating overlaps left 453 unique rejection-associated transcripts.[46]

TCMR Transcripts

We mapped the genes selectively expressed in TCMR in 703 biopsies by class comparison between histologic TCMR and everything else[78,79] (Table 3; Figure 5B). Each gene is shown on a volcano plot with the fold change on the y-axis and strength of association on the x-axis. Thousands of transcripts were differentially expressed in TCMR, reflecting infiltration by and activation of effector T cells, macrophages, and dendritic cells; IFNG-inducible transcripts; and weaker associations for inflammasome activation, innate immunity, and parenchymal injury. The top TCMR-selective transcripts by *P* value (shown in red) included transcripts expressed in activated effector T cells (*IFNG*, *LAG3*, and *SIRPG*), and activated macrophages and dendritic cells (*ADAMDEC1*, *CXCL13*, *CD86*, and *SLAMF8*). Some *IFNG*-inducible transcripts such as *ANKRD22* and *AIM2* were highly selective for TCMR, probably because they were induced by IFNG in macrophages recruited by TCMR. High expression of the *IFNG* gene itself is relatively selective for TCMR, even though IFNG-inducible genes are also increased in AMR and to a lesser extent in all injury. In pathway analysis, the top pathways included T cell receptor signaling and

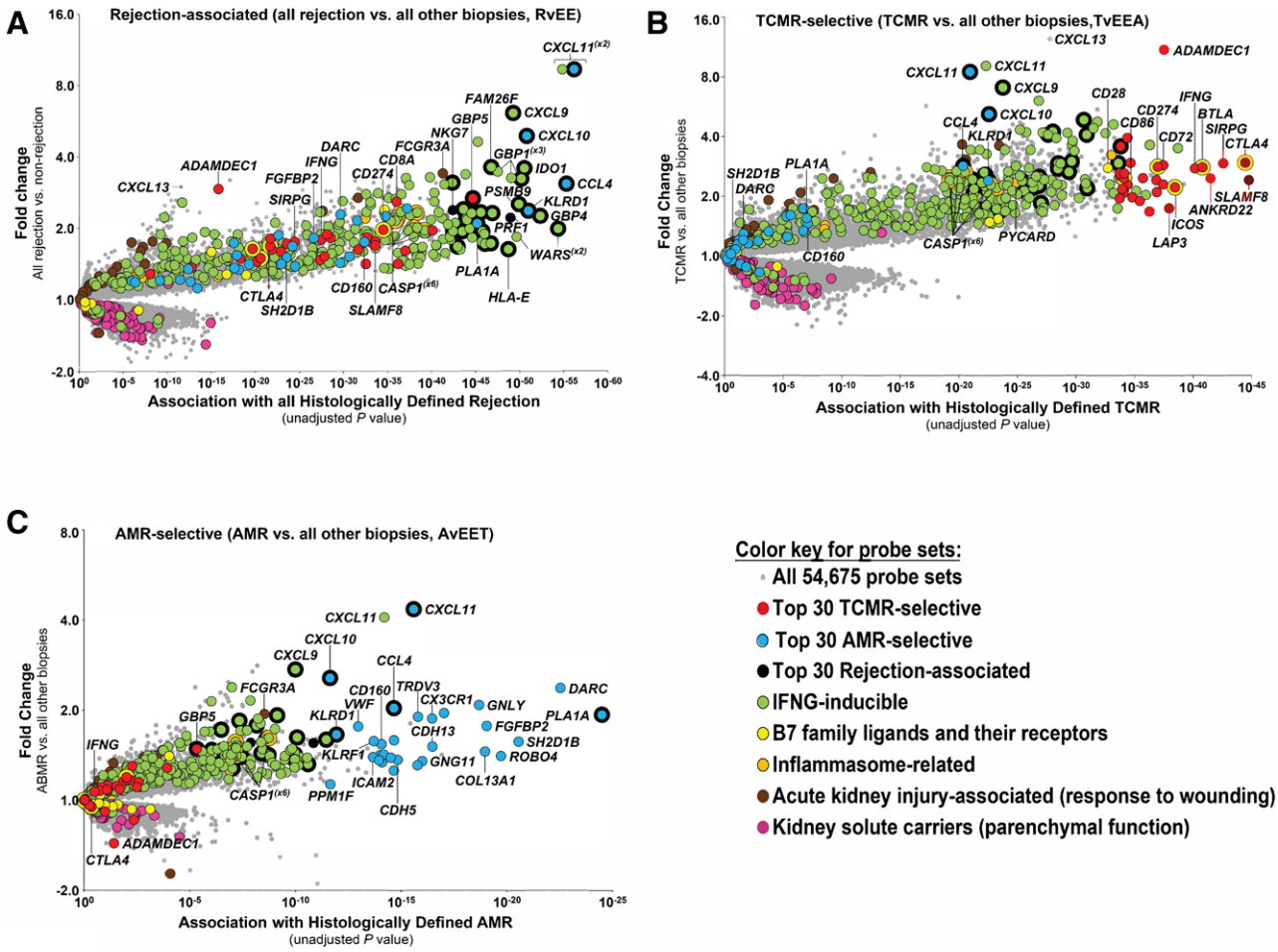

FIGURE 5. Landscapes of molecular rejection in kidney transplant biopsy populations shown as volcano plots.[47,79,80] Each transcript is shown as a point on the plot, colored by its annotation (if the annotation is available). Fold change of each transcript is shown on the y-axis, and association along the x-axis. Most significant transcripts will appear in the top right corner of each plot. The molecular landscapes of (A) all rejection, (B) TCMR, and (C) AMR. AMR, antibody-mediated rejection; TCMR, T cell–mediated rejection.

costimulation (Table 4).[79] These results suggest a model in which cognate effector T cells cross the kidney microcirculation, probably by recognition of donor antigen on dendritic cell processes,[82] and recruit and activate a team of myeloid cells and other lymphocytes to create a structured TCMR inflammatory compartment.

Some top TCMR-selective transcripts are regulatory checkpoints—for example, *CTLA4*, *LAG3*, and *SIRPG*[83]—but their expression correlates with *increased* TCMR intensity, not decreased intensity. Similarly, expression of transcription factor *FOXP3*, which is expressed in regulatory T cells,[84] is associated with rejection activity and inflammation, not with favorable outcomes.[85] The expression of these negative regulators in TCMR biopsies suggests that effector T cells in the tissue operate with their "brakes" partially applied, compatible with their mission in host defense of controlled purging of infectious agents without indiscriminate destruction of the life-sustaining organ.

AMR Transcripts

We mapped the genes selective for AMR in 703 kidney transplant biopsies by comparing histologic AMR to everything else[78,80] (Table 3; Figure 5C). The top transcripts selective for AMR (shown in blue) were expressed in NK cells (eg, adapter *SH2D1B*; cytotoxicity molecules granulysin (*GNLY*) and *FGFBP2*; and T-cell receptor delta *TRDC1*). Others were IFNG-inducible (eg, phospholipase *PLA1A* and chemokine *CXCL11*) or expressed in endothelial cells (eg, *ROBO4*, *DARC*, and cadherins *CDH5* and *CDH13*). AMR *activity* is associated with NK cell and IFNG-inducible transcripts (which strongly correlate with plasma dd-cfDNA[86]). The expression of some endothelial transcripts is decreased in AMR compared to normal kidney, for example, endothelial cell-specific molecule 1 (*ESM1*).[42] Pathways associated with AMR (Table 4)[87] suggest roles for vascular endothelial growth factors (which regulate *ESM1*); angiopoietin and leukocyte-endothelial interactions; and NK signaling, including evidence for CD16a Fc receptor signaling.

The prominence of NK cell transcripts in AMR suggested the potential role of antibody-dependent cell–mediated cytotoxicity[88] in AMR. Hidalgo et al[44] studied NK cell transcripts and immunostaining in biopsies from patients with known DSA status. Comparison of biopsies from DSA-positive versus DSA-negative patients found 132 transcripts significantly increased in association with DSA-positivity. Many were all-rejection transcripts, expressed in TCMR as well as AMR. Removal of transcripts shared with TCMR revealed 23 DSA-associated and AMR-"selective" transcripts (DSASTs), many expressed in NK

TABLE 3.

Top genes (sorted by *P* value) selectively *increased* in biopsies with TCMR, AMR, recent injury, and atrophy-fibrosis

TCMR		AMR		New/recent injury (IRRATs)		Atrophy-fibrosis	
Gene name	Gene Symbol	Gene name	Gene Symbol	Gene name	Gene Symbol	Gene name	Gene Symbol
ADAM-like, decysin 1	ADAMDEC1	Phospholipase A1 member A	PLA1A	Secretory leukocyte peptidase inhibitor	SLPI	Carboxypeptidase A3 (mast cell)	CPA3
Chemokine (C-X-C motif) ligand 13	CXCL13	Fibroblast growth factor binding protein 2	FGFBP2	Serpin peptidase inhibitor, clade A (alpha-1 antiproteinase, antitrypsin), member 3	SERPINA3	Chemokine (C-X-C motif) ligand 6	CXCL6
Signal-regulatory protein gamma	SIRPG	Granulysin	GNLY	Early growth response 1	EGR1	Membrane-spanning 4-domains, subfamily A, member 2 (FCER1B)	MS4A2
Janus kinase and microtubule interacting protein 1	JAKMIP1	SH2 domain containing 1B	SH2D1B	Olfactomedin 4	OLFM4	Gamma-aminobutyric acid A receptor, pi	GABRP
Inducible T-cell co-stimulator	ICOS	Sphingosine-1-phosphate receptor 5	S1PR5	Pentraxin 3, long	PTX3	tryptase alpha/beta 1	TPSAB1
Chemokine (C-X-C motif) receptor 6	CXCR6	Chemokine (C-X-C motif) ligand 11	CXCL11	Cathepsin S	CTSS	Fc Epsilon Receptor Ia	FCER1A
Zinc finger, BED-type containing 2	ZBED2	LY6	LYPD5	retinoic acid receptor responder (tazarotene induced) 1	RARRES1	Ceruloplasmin (ferroxidase)	CP
Cytotoxic T-lymphocyte-associated protein 4	CTLA4	T cell receptor delta constant	TRDC	lactotransferrin	LTF	Calpain 8	CAPN8
Interferon gamma	IFNG	Killer cell lectin-like receptor subfamily F, member 1	KLRF1	A kinase (PRKA) anchor protein 12	AKAP12	Cyclin D2	CCND2
Lymphocyte-activation gene 3	LAG3	Chemokine (C-C motif) ligand 4	CCL4	Peptidase inhibitor 15	PI15	Transmembrane protease, serine 4	TMPRSS4
SH2 domain containing 1A	SH2D1A	Guanylate binding protein 4	GBP4	ADAM metallopeptidase with thrombospondin type 1 motif, 1	ADAMTS1	Annexin A1	ANXA1
Basic leucine zipper transcription factor, ATF-like	BATF	Roundabout, axon guidance receptor, homolog 4 (Drosophila)	ROBO4	Multiple EGF-like-domains 11	MEGF11	Anterior gradient 3, protein disulfide isomerase family member	AGR3
B and T lymphocyte associated	BTLA	Chemokine (C-X3-C motif) receptor 1	CX3CR1	Oncostatin M receptor	OSMR	Chemokine (C-X-C motif) ligand 1 (melanoma growth stimulating activity, alpha)	CXCL1
CD8a molecule	CD8A	Perforin 1 (pore forming protein)	PRF1	Protein tyrosine phosphatase, receptor type, C	PTPRC	Frizzled-related protein	FRZB
CD8b molecule	CD8B	CD160 molecule	CD160	Ecotropic viral integration site 2A	EVI2A	Immunoglobulin kappa variable 1-27	IGKV1-27
T cell immunoreceptor with Ig and ITIM domains	TIGIT	Indoleamine 2,3-dioxygenase 1	IDO1	Transmembrane protein 252	TMEM252	Immunoglobulin heavy locus	IGH
Protein tyrosine phosphatase, nonreceptor type 7	PTPN7	Killer cell lectin-like receptor subfamily D, member 1	KLRD1	FBJ murine osteosarcoma viral oncogene homolog	FOS	Immunoglobulin kappa constant	IGKC
TOX high mobility group box family member 2	TOX2	Chemokine (C-X-C motif) ligand 9	CXCL9	Integrin, beta 3 (platelet glycoprotein IIIa, antigen CD61)	ITGB3	Immunoglobulin kappa locus	IGK
Src-like-adaptor 2	SLA2	Tryptophanyl-tRNA synthetase	WARS	Nicotinamide N-methyltransferase	NNMT	Tissue factor pathway inhibitor 2	TFPI2
SP140 nuclear body protein	SP140	Chemokine (C-X-C motif) ligand 10	CXCL10	Versican	VCAN	Annexin A1	ANXA1

AMR, antibody-mediated rejection; Ig, immunoglobulin; IRRAT, injury- and rejection-associated transcript; TCMR, T cell–mediated rejection.

TABLE 4.

Selected IPA pathways associated with molecular TCMR and AMR[79,81]

TCMR		AMR	
Pathway term name	**Adjusted *P***	**Pathway term name**	**Adjusted *P***
CTLA4 signaling in cytotoxic T lymphocytes (96)	1.9×10^{-7}	Natural killer cell signaling	3.6×10^{-6}
T cell receptor signaling (109)	1.9×10^{-7}	Fc epsilon RI signaling	2.1×10^{-3}
T helper cell differentiation (72)	5.5×10^{-7}	Granulocyte adhesion and diapedesis	3.6×10^{-6}
Communication between innate and adaptive immune cells (112)	6.6×10^{-5}	Agranulocute adhesion and diapedesis	5.0×10^{-6}
Primary immunodeficiency signaling (64)	1.4×10^{-4}	Angiopoietin signaling	1.2×10^{-3}
CD28 signaling in T helper cells (126)	8.1×10^{-4}	Caveolar-mediated endocytosis signaling	2.0×10^{-3}
Role of NFAT in regulation of the immune response (200)	1.4×10^{-3}	eNOS signaling	5.2×10^{-3}
iCOS-iCOSL signaling in T helper cells (126)	1.5×10^{-3}	Coagulation system	5.6×10^{-3}
Type I diabetes mellitus signaling (121)	1.5×10^{-3}	Nitric oxide signaling in the cardiovascular system	6.8×10^{-3}
PKC^{θ} signaling in T lymphocytes (144)	1.6×10^{-3}	VEGF family ligand-receptor interactions	1.0×10^{-2}

AMR, antibody-mediated rejection; TCMR, T cell–mediated rejection.

cells (eg, KLRF1 and MYBL1) or endothelium (eg, TEK and DARC). Biopsies with AMR had the highest DSAST expression. Immunostaining found NK-like cells (CD56+, CD68+, and CD3-negative) in peritubular capillaries, compatible with a role for NK cells in endothelial injury in AMR acting through CD16a.[80,89–91] These data support a model of AMR involving injury in the microcirculation induced by NK cells engaging endothelium-bound DSA through their CD16a Fc receptors.

Our concept of AMR involves the multimerization of Fc portions of immunoglobulin (Ig) G bound to the donor antigens on the endothelium.[92] NK cell CD16a Fc receptors binding to the distal hinge regions of the Fc multimers are then aggregated,[93] activating the zeta chain ITAMs. We assume that CD16a receptors assembled on the IgG Fc regions to resemble C1q.[92] FcR multimerization triggers zeta chain tyrosine phosphorylation and a calcium-calcineurin-NFAT signal that induces IFNG transcription and release of cytotoxic enzymes, similar to the processes in effector T cells activated by their T-cell receptors.[94] This interaction is modified by the effects of NK cell "self" receptors engaging their ligands (human leukocyte antigen class I-related) on the target tissue to sense "self" (inhibitory) or "missing self" (activating).[95] How the combination of CD16a signals and "missing self" signals interact in NK cells[96] must be unraveled.[35,96–103]

Understanding the mechanisms operating in AMR was initially difficult because mice do not manifest a similar AMR state, probably reflecting human-mouse differences in NK cells. Mice and humans developed from a common ancestor 100M y ago and inherited different NK systems. Unlike human NK cell CD16a, mouse NK cell CD16a Fc receptors do not associate with the zeta chain signaling apparatus.[90]

Developing Supervised TCMR and AMR Classifiers

We developed many classifiers, but for space limitations only the main TCMR and AMR classifiers are detailed below. A classifier for all rejection has been published.[64]

Development and Validation of a Molecular TCMR Classifier ($TCMR_{Prob}$)

We used machine learning to develop algorithms for diagnosing TCMR based on microarray results from 403 kidney transplant biopsies. The classifier trained on histologic TCMR assigned a score describing the probability of TCMR and its activity in each biopsy. The cross-validated scores correlated with histologic TCMR and its lesions (tubulitis and infiltrate).

For validation, a prospective study of new indication biopsies using the previously derived and locked classifier[104] demonstrated that the classifier identified TCMR biopsies in the new population as well as it did in the original population.

Development and Validation of a Molecular AMR Classifier (AMR_{Prob})

Beginning in 403 biopsies, we developed an AMR_{Prob} classifier trained on histologic AMR, similar to the TCMR classifier. The scores correlated with histologic AMR and its microcirculation lesions and DSA. Most biopsies with high classifier scores were called AMR by histology. High molecular AMR scores were strongly associated with graft loss in Cox regression analysis. The locked classifier developed in the discovery set identified AMR in the validation set.[105]

The AMR_{Prob} classifier showed that molecular AMR was frequently C4d-negative,[41,106] and that AMR was a more important cause of renal transplant loss than previously thought.[106,107]

Unsupervised Principal Component Analysis and Archetypal Analysis of Rejection

The above classifiers represent a supervised approach, trained on the histologic phenotypes. Following the ensemble principle, we developed an unsupervised approach based on the data structure rather than histology. We assessed molecular "rejection-ness" by combining 7 rejection classifiers (each an ensemble of 12 machine-learning methods) related to TCMR and AMR.[100] The rejection classifiers were those trained on the histologic diagnoses of AMR (AMR_{Prob}) or TCMR ($TCMR_{Prob}$) or the diagnostic histologic lesion scores: peritubular capillaritis (ptc)>0, g>0, cg>0, i>1, and t >1.

We distributed all biopsies in principal component analysis (PCA) based on their scores for 7 rejection classifiers in 1208 biopsies[61] and later in 1679 biopsies[108] (Figure 6). The distribution of PC scores formed a continuum in which

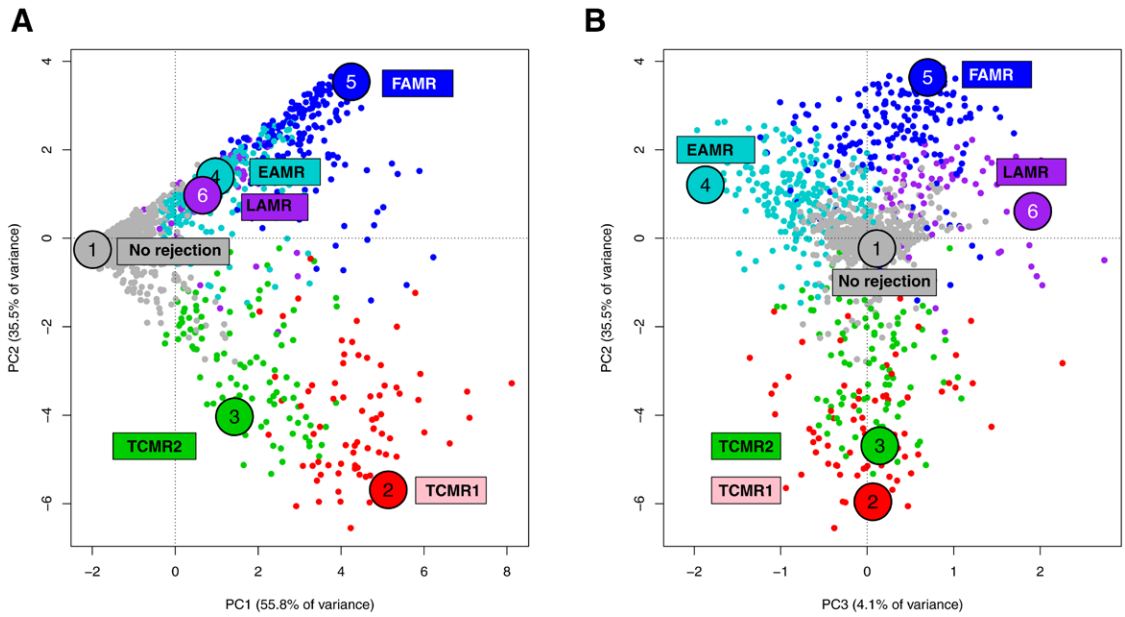

FIGURE 6. Visualizing archetypal groups in 1679 kidney transplant biopsies.[108] The 1679 biopsies are shown distributed by their rejection classifiers scores in PCA and colored by their archetype assignment, with y-axis PC2 and x-axis (A) PC1 or (B) PC3. (A, rejection increases with PC1, whereas PC2 separates TCMR from AMR). B, PC3 separates AMR stages but does not separate TCMR1 and TCMR2. AMR, antibody-mediated rejection; EAMR, early-stage AMR; FAMR, fully developed AMR; LAMR, late-stage AMR; PCA, principal component analysis; TCMR, T cell–mediated rejection.

PC1 represented all rejection; PC2 separated TCMR from AMR (Figure 6A), and PC3 separated AMR into early-stage, fully developed, and late-stage (Figure 6B).

Archetypal analysis generated 6 rejection archetype clusters: No rejection; TCMR1; TCMR2; Early-stage AMR (EAMR); Fully developed AMR (FAMR); and Late-stage AMR (LAMR). (The terms "early-stage" and "fully developed" AMR generally correspond to the Banff terms "active" and "chronic active" AMR.) These names reflect the disease state of the average members of each cluster, and should not be taken as meaning that every sample in a category belongs to a homogenous group.

TCMR1 was initially called "mixed" since ~60% of TCMR1 biopsies also had AMR features. However, we renamed the group TCMR1 to stress the intense TCMR activity in the group and to recognize that not all TCMR1 biopsies had AMR-like features. Compared to TCMR2, TCMR1 has on average more TCMR activity, AMR activity, DSA, and v-lesions, but less hyalinosis (suggesting under-immunosuppression—see below). Of interest, increased TCMR activity correlates with higher probability that early-stage AMR activity will also be present,[108] suggesting that intense effector T-cell generation in TCMR is often accompanied by generation of the T follicular helper T cells that are required to initiate DSA production.

Compared to TCMR1, TCMR2 has less activity but more fibrosis and hyalinosis, possibly because TCMR2 kidneys have had greater exposure to calcineurin inhibitors.[109] Most polyoma virus nephropathy (PVN) biopsies with molecular TCMR-like activity were TCMR2.

Further Details Related to Rejection

Type 1 Versus Type 2 AMR

AMR can occur either as an anamnestic DSA response in previously sensitized patients (type 1 AMR) or as a de novo DSA response (type 2 AMR).[110,111] We compared clinical features, histology, DSA, and gene expression in 205 biopsies with AMR: 103 (50%) type 1 and 102 type 2. Type 2 AMR was diagnosed much later and had more proteinuria, glomerular double contours, and AMR activity than type 1. Type 1 had superior graft survival compared with type 2 (63% versus 34% $P = 0.001$), suggesting that type 1 AMR in previously sensitized patients may go into remission more often than type 2 AMR because of de novo DSA production emerging in the context of immunosuppression. Type 1 versus type 2 AMR features are summarized in Figure 7.

Significance of Intimal Arteritis (v-lesions)

Although arterial lesions have long been regarded as predicting bad outcomes,[112,113] in multivariable analyses v-lesions were not strong predictors of survival compared to molecular injury.[108,114] Moreover, v-lesions can be caused by AMR or TCMR but also by injury, particularly in early biopsies.[64,115] The ambiguity of v-lesions can cause biopsies to be misinterpreted by histology.

Pure AMR (ie, with no TCMR) does not usually have arteritis: in 1679 biopsies, v-lesions were recorded in only 5% (20/387) of pure AMR biopsies,[116] primarily those with FAMR. Early severe type 1 AMR in patients with pre-existing DSA can produce arteritis,[117] but this entity is largely preventable and is now rarely seen outside of specialized centers undertaking high-risk sensitized transplants.

Isolated v-lesions without i- and t-scores are not usually due to TCMR: molecular TCMR scores were positive in only 21% of biopsies with isolated v-lesions compared to 95% of biopsies with i- and t-lesions as well as v-lesions.[64,115]

Chronic Active TCMR

The original Banff guidelines specified that tubulitis should not be assessed in tubules that were atrophic.[30]

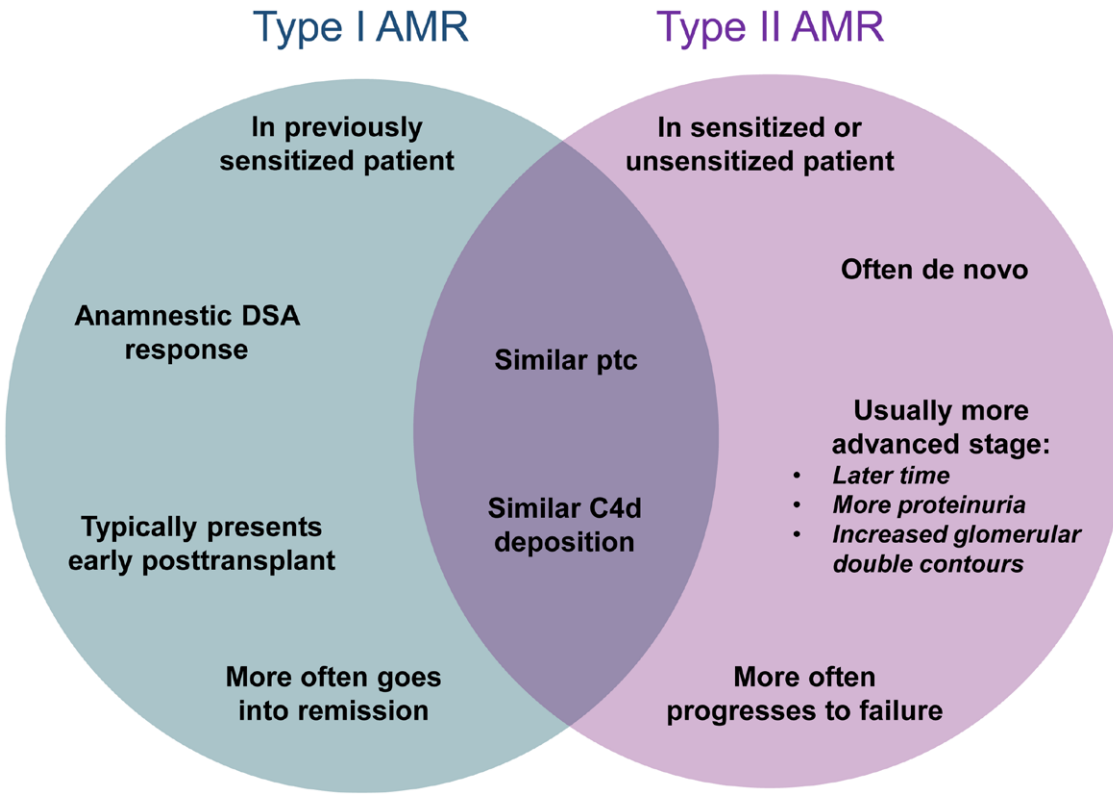

FIGURE 7. Venn diagram Type 1 vs Type 2 AMR. Characteristics of type 1 AMR are summarized on the left (blue) side of the Venn diagram, whereas characteristics of type 2 AMR are summarized on the right (purple) side. Features common to both type 1 and type 2 AMR are in the center. AMR, antibody-mediated rejection; DSA, donor-specific antibody; ptc, peritubular capillaritis.

However, late TCMR is associated with atrophy-fibrosis, which impairs tubulitis scoring. Naturally, this creates interest in diagnosing TCMR in the areas of atrophy-fibrosis. Inflammation in areas of atrophy-fibrosis—"i-IFTA"—is associated with an increased risk of failure,[118,119] but i-IFTA is also seen in primary renal diseases and may represent the inflammatory response to severe nephron injury rather than TCMR. Banff 2015[120] proposed criteria for defining chronic active TCMR based on inflammation and tubulitis in areas of atrophy-fibrosis, but MMDx analyses[121] and the DeKAF histologic analyses failed to support these criteria.[122,123] Banff 2017 revised this classification.[121–124] We recently confirmed that tubulitis is a robust feature of TCMR even in late biopsies with atrophy-fibrosis,[108] but the atrophy-fibrosis can make it difficult to score tubulitis.

TCMR Complexity in PVN

Many kidneys with PVN develop a TCMR-like process in addition to the injury process driven directly by the virus cytopathic effects.[60,125–127] The TCMR-like process in PVN is molecularly and histologically identical to TCMR in non-PVN biopsies. The TCMR-like changes usually emerge after immunosuppression has been reduced, permitting emergence of T cell immunity against viral antigens, alloantigens, or both.[128] We have shown that direct virus-induced injury and inflammation correlates with PVN viral mRNA and can be distinguished from TCMR-like activity, which correlates with the TCMR classifier.[125] The TCMR-like activity may resolve without treatment as the virus infection resolves, particularly after full immunosuppression is restored, but if it persists it can cause ongoing nephron damage and evolve into AMR.

To be clear, PVN is diagnosed by immunostaining of the biopsy, and the MMDx system assesses TCMR-like activity and parenchymal injury but does not make a direct diagnosis of PVN. Direct measurement of virus activity in the biopsy can be useful, for example, viral transcripts measured by RTPCR in the RNA isolated for the MMDx assay.[125] Following viremia is also a critical element in management.

Molecular Phenotype of Histologic "Borderline TCMR" Biopsies

Borderline TCMR changes, that is mild tubulitis and inflammation below the diagnostic cutoffs, represent a complex state that has implications for survival.[129] In 1679 INTERCOMEX biopsies, there were 128 histologic borderline biopsies: only 9 had molecular TCMR, whereas 24 had AMR, and most had no rejection.[116] Most histologic Borderline biopsies do not have molecular TCMR.

Molecular Features of AKI

The Injury- and Repair-associated Transcripts

The degree of recent parenchymal injury (AKI) and of nephron loss (atrophy-fibrosis) are strongly related to dysfunction and risk of graft failure.[130,131] To understand the molecular basis of AKI, we studied biopsies with no rejection taken in the first 6 wk, comparing biopsies with

dysfunction to pristine protocol biopsies with good function. This identified the IRRATs (Table 3).[48] Increased IRRAT expression correlated with depression of GFR at biopsy and with recovery of GFR in the follow-up period, whereas histologic lesions of "acute tubular injury" did not. IRRATs correlated with expression of many genes previously noted to be increased in AKI, for example, ITGB6, IL18, LCN2, and HAVCR1 (also known as kidney injury molecule 1[132]). The IRRATs were also related to transcripts previously annotated as induced by the transplantation process—donation-implantation injury—in mouse kidney isografts (ie, with no rejection): the injury-repair-induced transcripts (IRITs),[50,133] peaking at day 3 (IRITD3) or day 5 (IRITD5) posttransplant. Pathway analysis showed that the top injury-induced transcripts were associated with pathways related to cancer, "the wound that does not heal."[134] We also developed a classifier trained on the molecular changes in biopsies of kidneys with low eGFR (lowGFR$_{Prob}$), which correlates mainly with recent injury.[65]

Molecular Features of Irreversible Atrophy-fibrosis

We identified the transcripts that correlated with histologic atrophy-fibrosis lesions: immunoglobulin transcripts (IGTs) and B cell-associated transcripts,[51] and certain mast cell-associated transcripts. Mast cell-associated transcripts include the IgE Fc receptors A and B (*FCER1A, MS4A2*), carboxypeptidase 3 (*CPA3*),[66,135] and CXCL6[66] which is expressed in fibroblasts, mast cells, and endothelial cells. Many biopsies with atrophy-fibrosis also have increased expression of AKI-related IRRATs and increased risk of failure, reflecting recent or ongoing parenchymal injury (Table 3).[49,136]

Note that the IGTs reflect plasma cell infiltrates that accompany atrophy-fibrosis, and do not correlate with AMR activity. The DSA that causes AMR presumably originates in marrow plasma cells.

MMDx uses classifiers trained on interstitial fibrosis (the ci>1$_{Prob}$) and tubular atrophy (ct>1$_{Prob}$), and a classifier for proteinuria that correlated with chronic injury.[65]

THE MMDX REPORT

The above studies form the basis of the MMDx report expressing the rejection and injury states of each new biopsy (Figure 8). The key elements are:

1. The biopsy results are summarized by an expert reader, with comments on unusual features. MMDx can generate automated sign outs based on random forest predictions,[59] but we nevertheless have an expert review the report because some biopsies have multiple or ambiguous features or represent rare phenotypes.
2. The molecular scores are summarized for the inflammatory disturbance, AKI (the IRRAT score), atrophy-fibrosis (the ci>1$_{Prob}$ classifier, called the Fibrosis score on the report), and the all-rejection, TCMR, and AMR classifiers. (Note that the report abbreviates AMR as "ABMR", but we use "AMR" in this review as per journal policy.)
3. The archetype scores are summarized. Archetype scores are proportions, unlike binary classifier scores. Thus, a biopsy assigned to a particular rejection archetype cluster can have high scores in 2 different archetypes but is only assigned to 1 group based on its highest ("dominant") archetype score. We rely on the binary classifier scores to interpret these cases. For example, intense TCMR1 often has elevated binary AMR$_{Prob}$ activity as well. As stated earlier, there is no "Mixed" archetype group per se: we assess the extent of TCMR and AMR separately.
4. The rejection classifier scores are used to visualize the relationship of a new biopsy (triangle) to the biopsies in the locked reference set, which are colored by their rejection archetype states and shown in PCA plots: PC2 versus PC1 (left panel) and PC2 versus PC3 (right panel).
5. The percent cortex is estimated by *NPHS2* (podocin) expression, because low %cortex can affect some scores, for example, inflammation, cg-classifier, and late-stage AMR, and will always be noted as a caveat on the report.
6. Selected rejection and injury scores for the new biopsy are compared to relatively normal biopsies.
7. The characteristics of this biopsy are compared to its nearest neighbors in the reference set.

Histology-MMDx Discrepancies

Some disagreement exists between MMDx and histology as expected for any 2 independent diagnostic systems (Table 5). In 1679 biopsies, there were ~37% discrepancies, about half with potential to affect therapy. Disagreement was ~20% in no rejection and in AMR, but higher in TCMR (about 40%). In our previous analyses, histologic TCMR was particularly subject to interpathologist disagreement[60]: among 3 pathologists each had about 50% sensitivity for TCMR diagnoses by another pathologist.[60] Very high and low molecular scores corresponded with unanimity among 3 pathologists (Figure 9), recalling the concept of ensemble assessment. Thus, some disagreement with histology was expected from the known "noise" in single-observer histology assessments.[116] MMDx is precise in assessing an individual sample, but both MMDx and histology are affected by sampling variation, for example, medulla versus cortex.[72] While making no claim that MMDx is perfect, we have outlined reasons for confidence in MMDx when it disagrees with histology.[12,59] For example, MMDx findings correlate more strongly with dd-cfDNA, function, and survival than histology.[4,86]

Some discrepancies between histology and MMDx reflect different conventions. As noted above, histology will generally not diagnose TCMR despite tubulitis and interstitial infiltrate when PVN is present, whereas MMDx recognizes TCMR but does not specify whether it is due to alloantigens, polyoma virus antigens, or both.[125] Additionally, histology will call late-stage AMR cg whereas MMDx often calls this LAMR.

RECENT DEVELOPMENTS IN MMDX STUDIES

The MMDx project raised many issues about the processes that occur in the kidney transplant population. From these findings, we continue to focus in particular on 5 issues: nonadherence, DSA-negative AMR, "what lies beneath" our threshold for diagnosing rejection, the relationship between rejection and injury, and time relationships.

Under-immunosuppression and Nonadherence

We previously studied medical records of kidney transplants that progressed to failure and focused on those in which the failure was attributed to rejection (Figure 10).

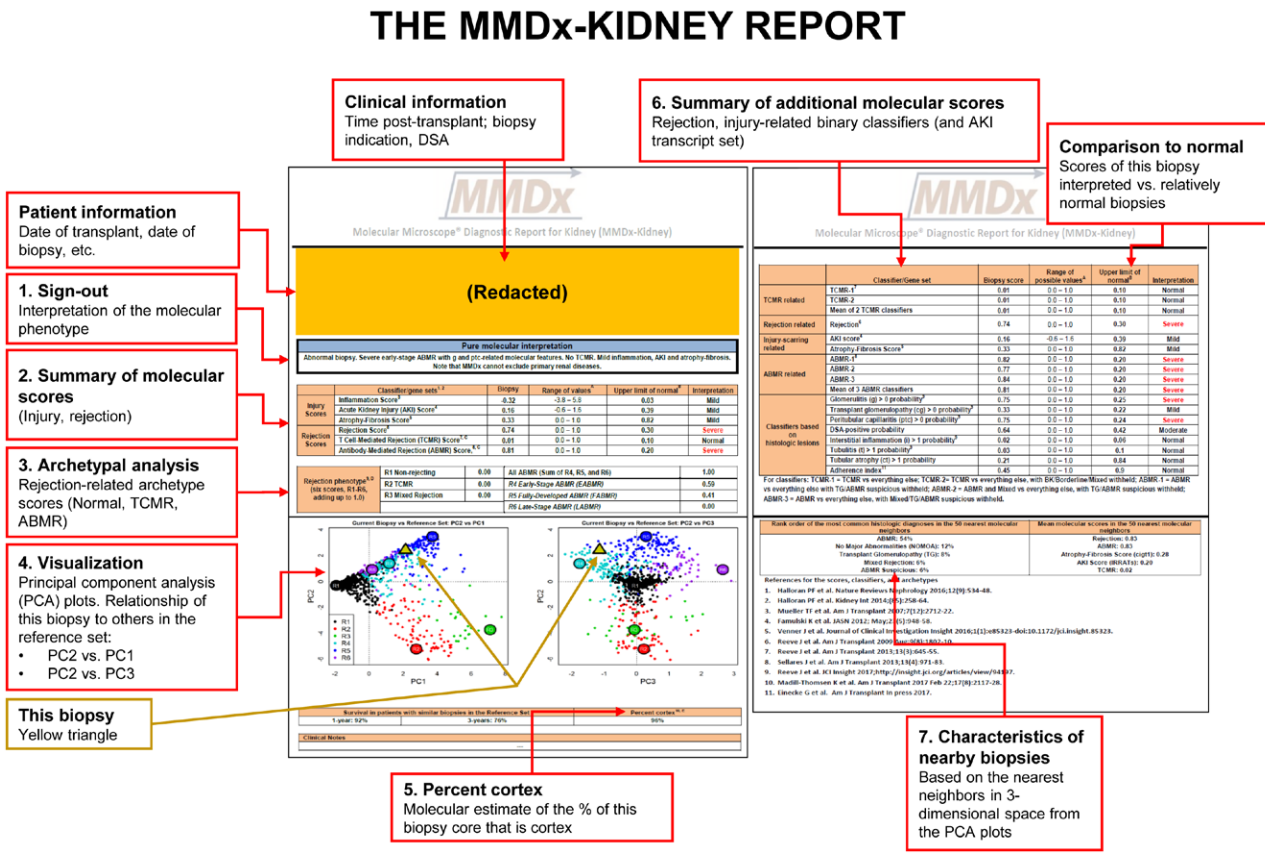

FIGURE 8. The MMDx-Kidney report. Numbered items on the report are as follows: (1) The biopsy results are summarized by an expert reader, with comments on unusual features. This remains a necessary step because some biopsies have multiple or ambiguous features or rare phenotypes. (2) The molecular scores are summarized for the inflammatory disturbance, AKI (IRRAT), atrophy-fibrosis (the ci-classifier), and the all-rejection, TCMR, and AMR classifiers. (3) The archetype scores are summarized. Archetype scores are proportions, unlike binary classifier scores. Thus, a biopsy assigned to a particular archetype rejection cluster can have nearly as high a score in a second archetype but is only assigned to 1 group based on its highest ("dominant") archetype score. (4) The rejection classifier scores are used to locate the position of the new biopsy (triangle) in relationship to the biopsies in the locked, N = 1208 reference set, which are colored by their rejection archetype states and shown in PCA plots: PC2 versus PC1 (left panel) and PC2 versus PC3 (right panel). (5) The percent cortex is estimated by *NPHS2* (podocin) expression. Low %cortex (<10%) can affect some scores, eg, inflammation, cg-classifier, and late-stage AMR. (6) Details of selected rejection and injury scores of interest are presented and compared to relatively normal biopsies. (7) The characteristics of this biopsy are compared to its nearest neighbors in the reference set. AKI, acute kidney injury; AMR, antibody-mediated rejection; cg, transplant glomerulopathy; IRRAT, injury- and rejection-associated transcript; MMDx, Molecular Microscope Diagnostic System; PCA, principal component analysis; TCMR, T cell–mediated rejection.

Nonadherence concerns were recorded in about half of the patients whose kidney failed because of rejection.[127]

In patients biopsied at the time of *recent* or *current* nonadherence, the biopsy typically shows TCMR1, often with emerging AMR activity. In clinical experience, such cases may progress to AMR after the TCMR is treated.

Hyalinosis is a feature of calcineurin inhibitor (CNI) therapy and develops with adequate exposure to CNIs over time. As noted above and in Table 6, low afferent arteriolar hyalinosis scores was common in biopsies with TCMR,[137–139] particularly TCMR1, suggesting that underimmunosuppression or nonadherence is a common trigger for TCMR. However, hyalinosis is difficult to interpret because it can be caused by conditions other than CNIs (eg, donor aging, glomerular diseases, and atrophy-fibrosis).

DSA-negative AMR

Molecular AMR assessed by MMDx is often in DSA-negative patients (Table 6),[61] associated with typical microvascular inflammation.[140] We analyzed the features of DSA-negative AMR within the 1679 biopsy population,[42] comparing 150 DSA-negative AMR to 248 DSA-positive AMR.[42] DSA-positive AMR had a later median time posttransplant (3.9 y) than DSA-negative AMR (median 2.4 y). DSA positivity increased as AMR became fully developed, then declined: EAMR, 56% positive; FAMR, 70% positive; and LAMR, 58% positive. DSA-negative AMR had lower mean molecular intensity and ptc scores, but slightly more injury and lower eGFR, compatible with its earlier time posttransplant. However, the transcripts associated with AMR were virtually identical in DSA-negative and DSA-positive AMR, whether assessed by fold change (Figure 11A) or *P* value (Figure 11B). Graft loss was similar in DSA-negative and DSA-positive AMR. The findings were similar in a new biopsy population in the Trifecta study[141] (see below). In summary, compared to DSA-positive AMR, DSA-negative AMR is usually C4d-negative, less fully developed, and on average slightly earlier, but involves the same molecular mechanisms, releases as much dd-cfDNA, and carries a similar risk of failure.

TABLE 5.

Relating histologic rejection diagnoses to Expert1MMDx rejection sign-out comments (6 classes, N = 1679)

			Histologic diagnoses (6 classes)									
			Rejection-related, N = 740									
			AMR-related, N = 417				TCMR-related, N = 267					
				pAMR								
			AMR	AMR suspicious	CG	Mixed, N = 56	TCMR	pTCMR (borderline)	No rejection	No rejection excluding PVN*a*	Row totals	No. discrepancies per row (%)
Expert1MMDx sign-out comments (6 class)	AMR-related, N = 561	AMR	**260**	**17**[b]	**32**[b]	**25**[c]	**20**[d]	**24**[d]	**131**[d]	**(127)**	**509**	**249/509 (49%)**
		Possible AMR	**12**[b]	1	1	**1**[c]	**3**[d]	5[d]	**29**[b]	(26)	52	50/52 (96%)
	Mixed		**6**[c]	**2**[c]	**1**[c]	**22**	**25**[c]	**4**[c]	**9**[c]	**(8)**	**69**	**47/69 (68%)**
	TCMR-related, N = 144	TCMR	**5**[d]	**0**	**1**[d]	**5**[c]	**55**	**9**[b]	**48**[d]	**(22)**	**123**	**68/123 (55%)**
		Possible TCMR	**0**	0	0	**1**[c]	**8**[b]	3	**9**[b]	(6)	21	18/21 (86%)
	No rejection		**50**[d]	**13**[b]	**16**[b]	**2**[c]	**28**[d]	**83**[b]	**713**	**(698)**	**905**	**192/905 (21%)**
Column totals			**333**	33	51	**56**	**139**	128	**939**	(887)	1679	624/1679 (37%)
No. discrepancies per column (%)			**73/333 (22%)**	32/33 (97%)	50/51 (98%)	**34/56 (61%)**	**84/139 (60%)**	125/128 (98%)	**226/939 (26%)**	189/887 (21%)	624/1679 (37%)	

pTCMR and pAMR were ignored in definite AMR or TCMR respectively. Twenty-six Expert1MMDx TCMR/Histology NR were PVN virus positive.
Bolding indicates clear rejection/no rejection categories.
[a] Excludes PVN from row totals. Histology usually does not diagnose TCMR in biopsies with PVN; MMDx recognizes molecular TCMR regardless of PVN status, but acknowledges that it does not distinguish whether the TCMR activity is directed against alloantigens, PVN antigens, or both.
[b] Boundary discrepancies between Expert1MMDx and histology (N = 228).
[c] Mixed discrepancies between Expert1MMDx and histology (N = 81).
[d] Clear discrepancies between Expert1MMDx and histology (N = 315).
AMR, antibody-mediated rejection; cg, transplant glomerulopathy; MMDx, Molecular Microscope Diagnostic System; PVN, polyoma virus nephropathy; TCMR, T cell–mediated rejection; TG, transplant glomerulopathy.

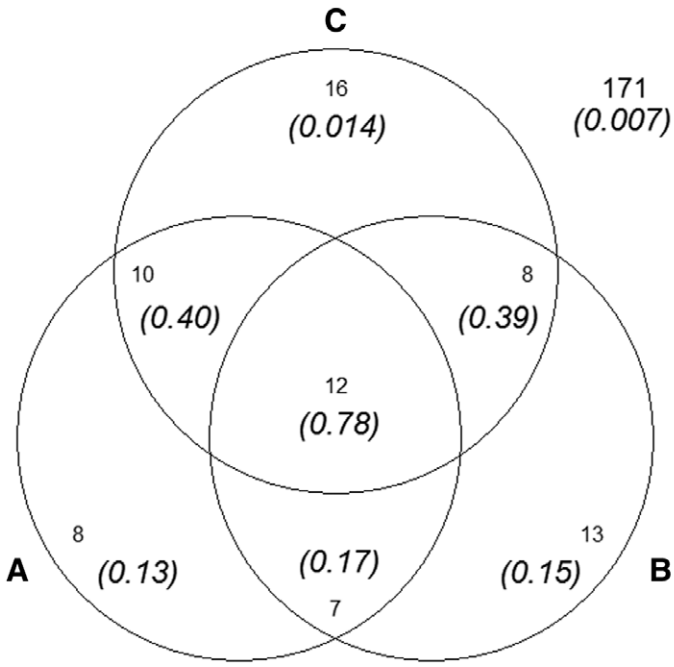

Votes for TCMR (number of biopsies)	Mean TCMR score
0/3 (171)	0.007
1/3 (16,8,13)	0.10
2/3 (10,8,7)	0.32
3/3 (12)	0.78

FIGURE 9. Venn diagram showing the relationship between the molecular TCMR score and the agreement among 3 pathologists ("A," "B," and "C") in the 245 biopsy subset.[60] Numbers in italics show the average molecular TCMR score in the biopsies. Numbers with no parentheses are the intersections of the number of biopsies diagnosed as TCMR by the 3 pathologists. One hundred seventy-one biopsies were called no TCMR by all 3 pathologists (mean TCMR score of 0.007, numbers outside of the diagram). Biopsies with either i2t2 TCMR or mixed rejection were considered TCMR. Isolated v-lesion TCMRs were not counted as TCMR. AMR, antibody-mediated rejection; TCMR, T cell–mediated rejection.

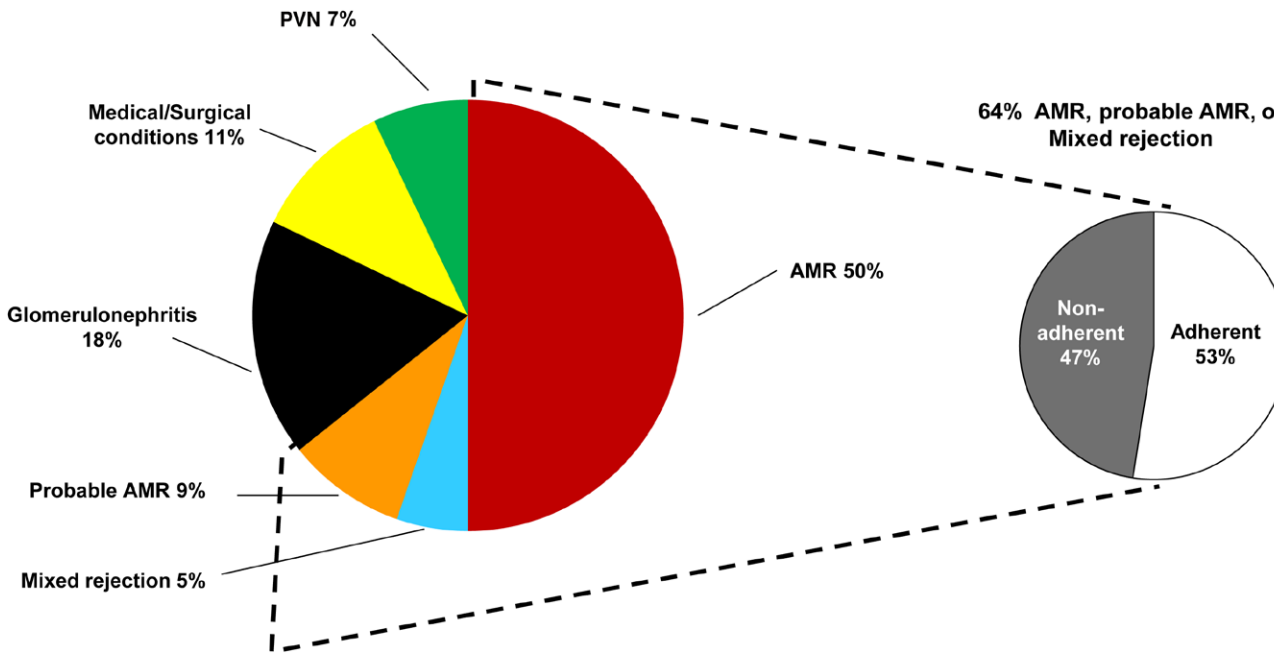

FIGURE 10. Attributed causes of graft failure in the biopsy-for-cause population—60 losses in 315 patients with follow-up.[127] Distribution of the attributed causes of failure. Failures that could not be attributed due to missing clinical information are not represented (N = 4). AMR, antibody-mediated rejection; PVN, polyoma virus nephropathy.

The many possible explanations for DSA-negative AMR have been discussed elsewhere, and there may be different explanations in different cases.[42] At present, our working hypothesis for the majority of DSA-negative AMR cases is that the human leukocyte antigen antibodies causing AMR are undetectable in plasma because they are completely absorbed by the kidney. DSA will only be demonstrated in plasma when production rates exceed the ability of the kidney to absorb it, which is most likely to occur in FAMR.

"What Lies Beneath": Minor AMR-like Changes in Biopsies Considered "No Rejection"

We explored the significance of subtle AMR-like changes in gene expression in biopsies that histology and

TABLE 6.

Clinical variables, histologic lesion scores, and molecular features in the kidney rejection and injury archetype clusters

		Mean value or score in each archetype					
		Rejection archetypes (N=1679)					
Variable		**No rejection (N = 1040)**	**TCMR1 (N = 75)**	**TCMR2 (N = 100)**	**EAMR (N = 210)**	**FAMR (N = 182)**	**LAMR (N = 72)**
Mean transcript set scores							
TCMR-related	QCAT	0.62	**2.53**	2.04	1.25	1.46	1.23
AMR-related	DSAST	0.07	0.33	0.17	0.49	**0.89**	0.37
	NKB	0.36	1.01	0.80	1.07	**1.50**	0.85
Recent injury-related	FICOL	1.11	**1.61**	1.58	0.90	1.03	1.21
	IRITD3	0.04	**0.22**	0.17	0.06	0.12	0.14
	IRITD5	0.33	**0.64**	0.59	0.37	0.47	0.50
	IRRAT	0.26	**1.13**	0.99	0.38	0.50	0.59
Atrophy-fibrosis	IGT	0.60	1.94	**2.27**	1.02	1.38	1.64
Mean molecular classifier scores							
TCMR-related	i-score ($i > 1_{Prob}$)	0.06	**0.84**	0.65	0.10	0.15	0.14
	t-score ($t > 1_{Prob}$)	0.06	**0.83**	0.62	0.10	0.13	0.11
	TCMR ($TCMR_{Prob}$)	0.03	**0.60**	0.24	0.05	0.06	0.05
AMR-related	AMR (AMR_{Prob})	0.08	0.30	0.13	0.37	**0.74**	0.25
	Glomerular double contours ($cg > 0_{Prob}$)	0.09	0.30	0.15	0.21	**0.68**	0.56
	Peritubular capillaritis ($ptc > 0_{Prob}$)	0.15	0.71	0.47	0.62	**0.77**	0.49
	Glomerulitis ($g > 0_{Prob}$)	0.18	0.47	0.27	0.60	**0.81**	0.45
Rejection-related	Rejection (Rej_{Prob})	0.12	**0.85**	0.54	0.59	0.80	0.48
Recent injury-related	$lowGFR_{Prob}$	0.32	0.60	0.52	0.30	0.34	0.42
Atrophy-fibrosis	ci-score ($ci > 1_{Prob}$)	0.31	0.40	0.53	0.35	0.44	0.58
Mean clinical features							
Clinical	Median time of biopsy posttransplant (d)	371	258	506	724	1482	**2744**
	GFR (cc/min)	44	30	36	**50**	43	32
	Proteinuria[a]	0.55	0.58	0.51	0.58	**0.78**	0.77
	Donor age (y)	**46**	40	41	**46**	39	39
	Recipient age (y)	**52**	46	48	51	47	47
Mean histology features							
AMR lesions and DSA status	g (glomerulitis)	0.24	0.48	0.19	1.09	**1.64**	0.84
	ptc (capillaritis)	0.25	1.04	0.58	1.10	**1.82**	1.03
	cg (double contours)	0.19	0.11	0.08	0.49	1.42	**1.67**
	%DSA-positive of tested	34%	41%	33%	56%	70%	**58%**
TCMR lesions	i (interstitial infiltrate)	0.40	**2.21**	1.97	0.64	0.65	0.74
	t (tubulitis)	0.33	**2.23**	1.99	0.46	0.46	0.46
Rejection lesions	v (vasculitis)	0.02	**0.46**	0.13	0.06	0.15	0.08
Atrophy-fibrosis-related	ci (fibrosis)	1.11	1.10	**1.74**	1.26	1.66	1.62
	ct (atrophy)	1.04	1.04	**1.70**	1.03	1.45	1.51
	cv (fibrous intimal thickening)	0.95	0.60	1.07	0.81	**1.20**	1.00
	ah (hyalinosis)	1.01	0.21	0.70	1.00	1.31	**1.75**

Bolding indicate the highest value per row.

[a] Proteinuria is coded as positive = 1, negative = 0. Therefore, the means for these variables indicate the fraction of biopsies that were positive. Missing values were excluded from the calculations.

AMR, antibody-mediated rejection; cg, transplant glomerulopathy; DSA, donor-specific antibody; DSAT, DSA-selective transcripts; EAMR, early-stage AMR; FAMR, fully developed AMR; FICOL, fibrillar collagen; g, glomerulitis; GRIT, IFNG-inducible transcripts; i, interstitial inflammation; IGT, immunoglobulin transcripts; IRITD3, Injury-repair induced, day 3; IRITD5, Injury-repair induced, day 5; IRRAT, injury- and rejection-associated transcript; LAMR, late-stage AMR; M, molecular classifier scores; NKB, NK cell burden; QCAT, cytotoxic CD8 T cell-associated transcript; ptc, peritubular capillaritis; S, archetype score; t, tubulitis; TCMR, T cell–mediated rejection.

MMDx classified as no rejection. As an additional tool for these analyses, we developed a DSA-probability classifier (DSA_{Prob}), which correlated with the AMR_{Prob} classifier because it too was detecting the AMR-related changes in the biopsies. When we visualized the distribution of classifier scores in the 1679 biopsy cohort (Figure 12A), we found a gradient in DSA_{Prob} (Figure 12B) and AMR_{Prob} (Figure 12C) scores that extended into biopsies classified

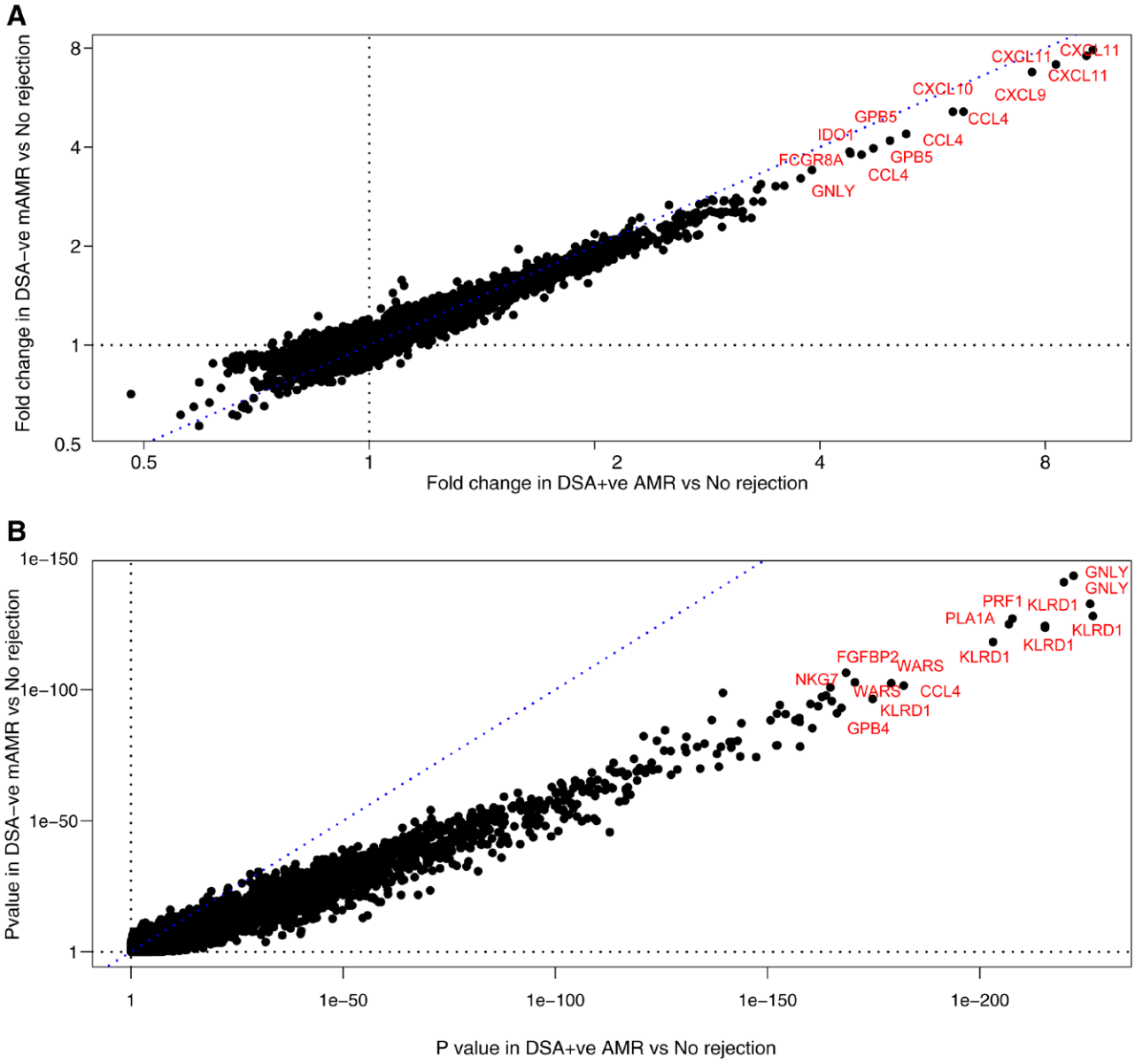

FIGURE 11. Genes associated with DSA-positive AMR.[42] Scatterplots showing (A) fold change in DSA-negative mAMR biopsies versus no rejection biopsies (y-axis) plotted against fold change in DSA-positive mAMR biopsies versus no rejection biopsies (x-axis); (B) *P* values for the same class comparisons. AMR, antibody-mediated rejection; DSA, donor-specific antibody.

as no rejection using our current thresholds. No rejection biopsies that were DSA-positive had higher DSA_{Prob} and AMR_{Prob} classifier scores—that is, subtle AMR-related molecular changes. High AMR_{Prob} and DSA_{Prob} scores predicted impaired survival in no rejection biopsies, whereas DSA status did not. These findings have recently been confirmed.[74] Thus, subtle AMR stresses are operating in some kidneys previously considered to have no rejection.

Similar analysis of subtle low-level TCMR changes is in progress. These need to take into account that effector memory T cells can enter damaged tissue even when there is no TCMR.[142]

These findings raise the question: what is rejection, and where should we draw the boundaries between positive and negative classes? Like all disease definitions, we have defined AMR and TCMR with arbitrary cutoffs and these should be reassessed, probably based on implications for clinical management, for example, where treatment would be beneficial.

Rejection–Injury Relationships

We found distinct relationships between the rejection archetype groups and the parenchymal injury states (Figure 13).

Molecular measures of AKI (Figure 13A and B) were consistently high in both TCMR1 and TCMR2.

Measures of atrophy-fibrosis (Figure 13C and D) were increased in TCMR2, because fibrosis is a feature of TCMR2 even in the first year posttransplant.[108] Fibrosis was also increased in FAMR and LAMR because of nephron loss.

Histologic fibrous intimal thickening in small arteries was increased most in groups with fibrosis (TCMR2, FAMR, and LAMR) but was particularly increased in FAMR, indicating that AMR directly affects small arteries (Figure 13E).

Hyalinosis scores were very low in TCMR1 biopsies as noted earlier, and slightly low in TCMR2 (Figure 13F).

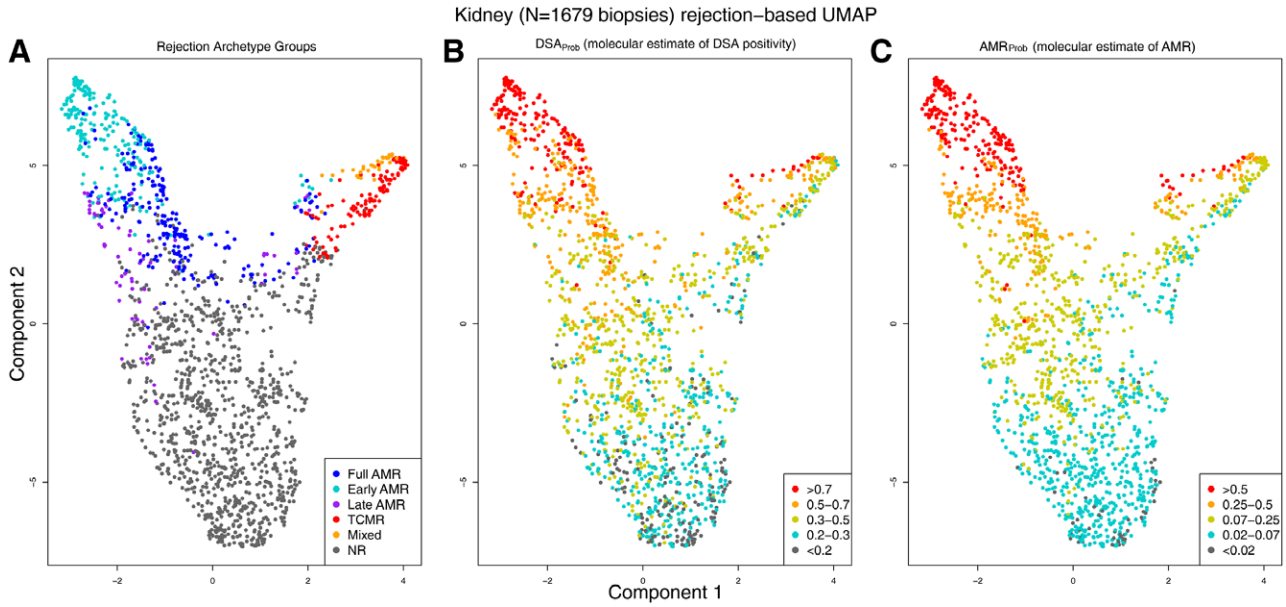

FIGURE 12. UMAP projections of 1679 biopsies.[63] All 1679 indication kidney transplant biopsy specimens, shown using UMAP, colored by (A) assigned rejection-based archetypal class, (B) increasing DSA_{Prob} classifier score, and (C) increasing AMR_{Prob} score. Biopsy samples with low probability of molecular rejection are located toward the bottom of Component 2 in all panels. Biopsy samples with rejection are located toward the upper region of Component 2, with AMR on the left and TCMR on the right of Component 1. AMR, antibody-mediated rejection; DSA, donor-specific antibody; TCMR, T cell–mediated rejection.

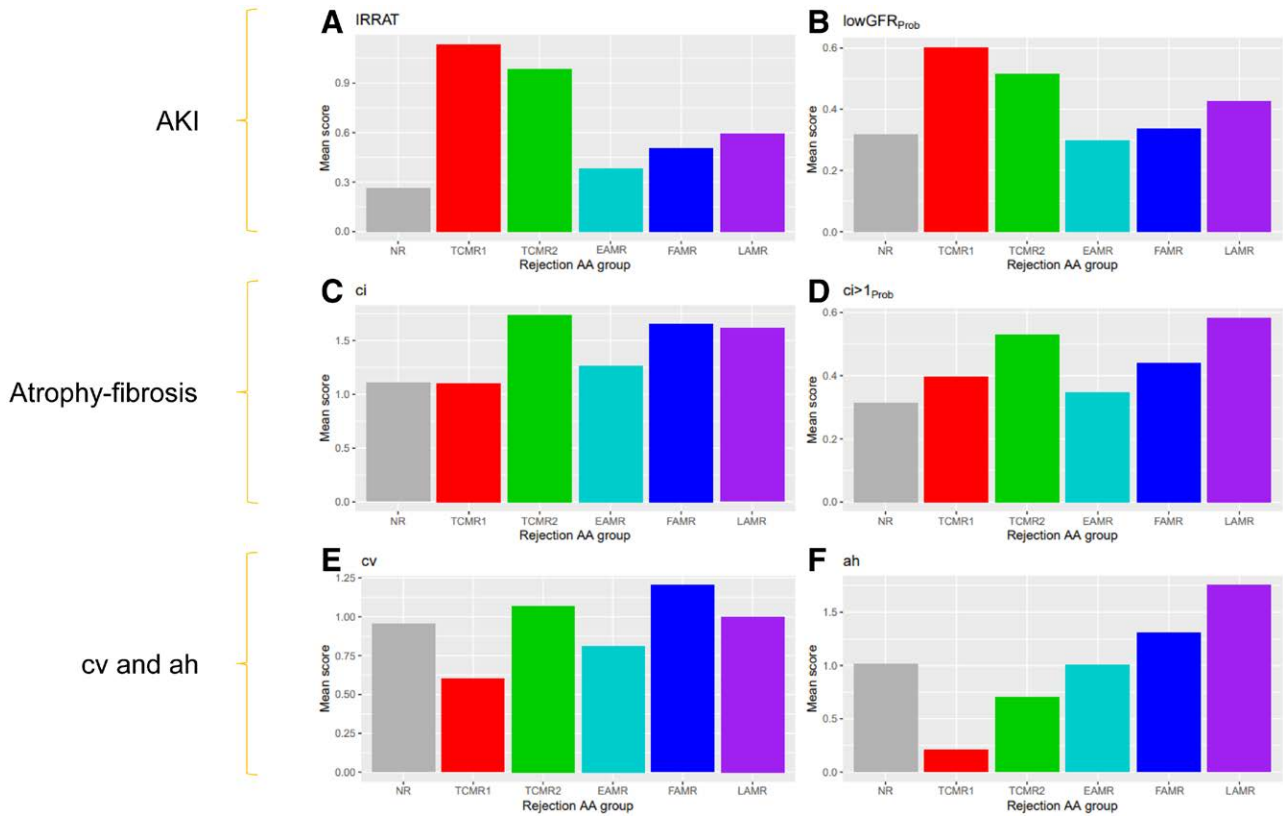

FIGURE 13. Bar plots showing the mean scores for molecular or histologic variables in each rejection archetypal analysis cluster in 1679 biopsies. Scores shown are injury-related, that is, (A) IRRAT and (B) $lowGFR_{Prob}$ classifier scores, atrophy-fibrosis related, that is, (C) ci-lesion scores or (D) ci > 1_{Prob} classifier scores, (E) related to arteritis, that is, cv-lesion score, or (F) related to underhyalinosis, that is, ah lesion score. AKI, acute kidney injury; EAMR, early-stage antibody-mediated rejection; FAMR, fully developed antibody-mediated rejection; GFR, glomerular filtration rate; IRRAT, injury- and rejection-associated transcript; LAMR, late-stage antibody-mediated rejection; NR, no rejection; TCMR, T cell–mediated rejection.

Associations With Time Posttransplant

Time posttransplant has a striking relationship to the rejection and injury phenotypes in kidney transplant biopsies (Figure 14). In Figure 14A, the proportion of biopsies with MMDx diagnosis of TCMR rises after the first 2 mo posttransplant, plateaus at just <1 y, steadily declines after 2–3 y, and is rare after 10 y. There are a few early cases of AMR, presumably type 1. The incidence of AMR rises after 1 y and is sustained. Figure 14B shows the proportion of biopsies in each archetype group. Both

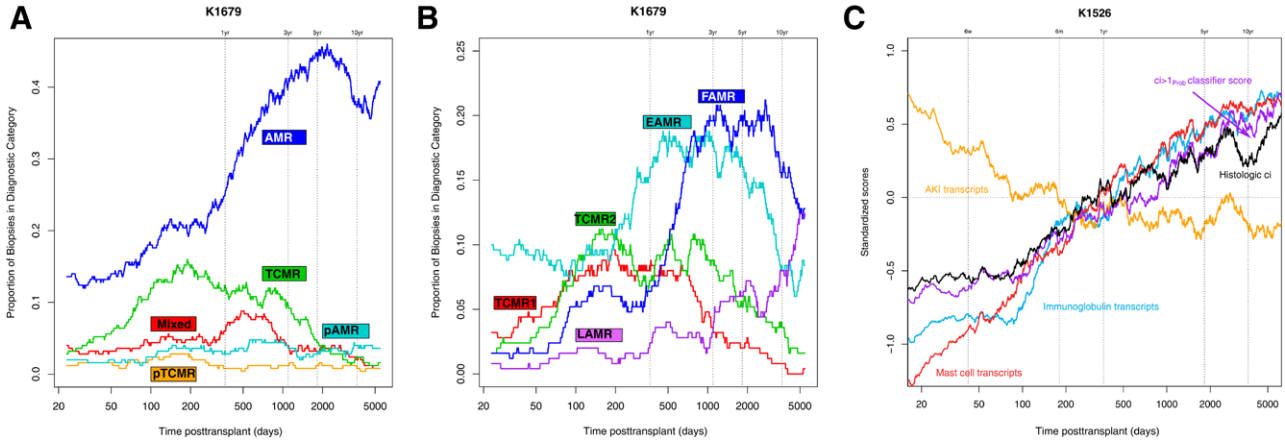

FIGURE 14. Moving average plots showing the proportion of biopsies assigned to particular diagnostic categories and selected molecular scores over time posttransplant (d).[66] Biopsies are categorized according to (A) MMDx sign-outs or (B) archetypal analysis clusters within all 1679 biopsies. (C) Standardized scores from 1526 biopsies are shown (1679 biopsies with low-cortex samples removed = 1526). As there are large differences in mean scores between scores, all scores were standardized to a mean of 0.0 before plotting. The y-axis is in standard deviation units. Biopsies sorted by ascending time of biopsy posttransplant. A line for histologic ci-lesions is shown for comparison to the molecular scores. Window size for averaging is 100 biopsies. AMR, antibody-mediated rejection; EAMR, early-stage AMR; FAMR, fully developed AMR; LAMR, late-stage AMR; MMDx, Molecular Microscope Diagnostics System; TCMR, T cell–mediated rejection.

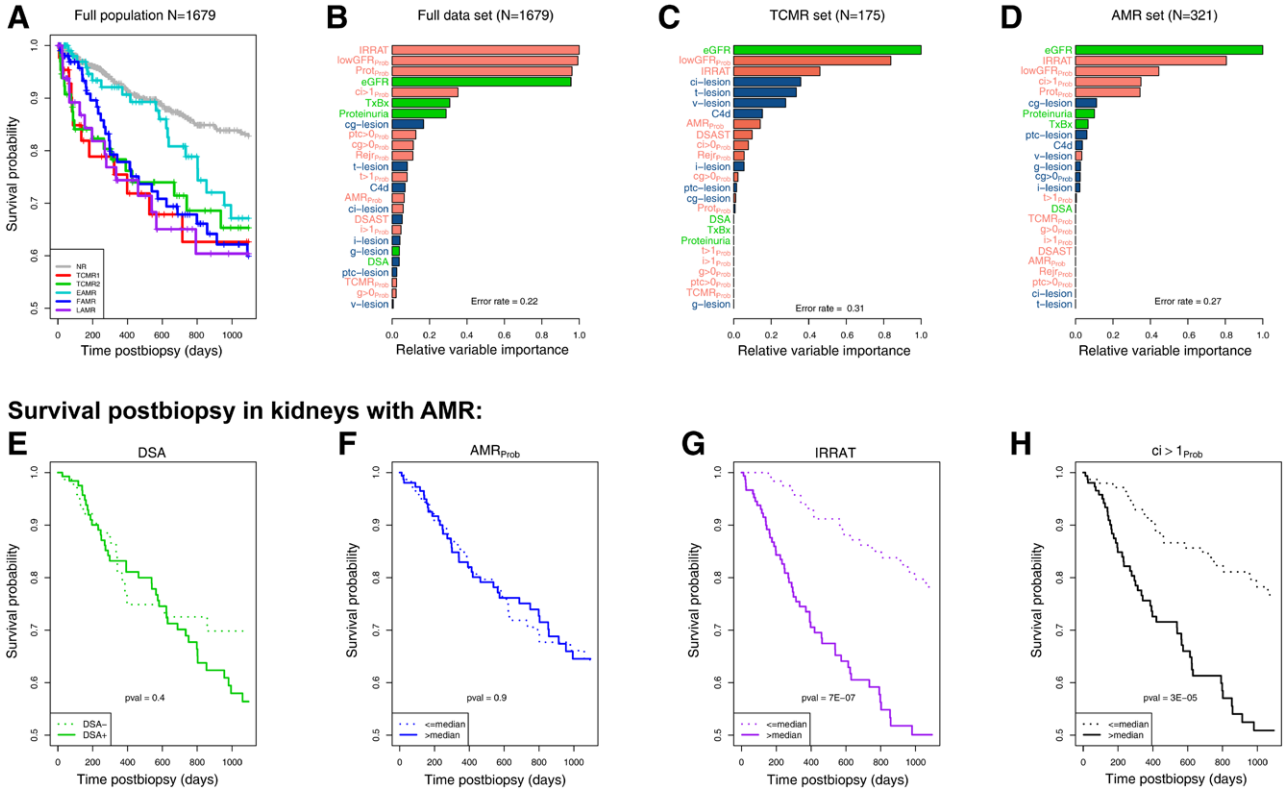

FIGURE 15. Various relationships between molecular, histological, and clinical variables and graft survival postbiopsy.[108,114] (A) Survival shown per archetype group in 1679 biopsies. B–D, Relative variable importance in random survival forest analysis in (B) all biopsies (N = 1679), (C) biopsies with molecular TCMR (N=175), and (D) biopsies with molecular pure AMR (N = 321). E–H, Association with survival within MMDx pure molecular AMR samples. Graft survival is shown in relation to: (E) DSA status (DSA-positive versus DSA-negative) and (F) AMR_{Prob} score (expression above or below the median). For comparison, we show the impact of 2 strong predictors of graft loss: (G) the molecular AKI score (IRRAT score) and (H) the molecular atrophy-fibrosis score (ci > 1_{Prob}, expression above or below the median). AKI, acute kidney injury; AMR, antibody-mediated rejection; DSA, donor-specific antibody; IRRAT, injury- and rejection-associated transcript; TCMR, T cell–mediated rejection.

TCMR1 and TCMR2 rise, plateau, and decline more or less in parallel. Thus the TCMR1-TCMR2 gradient is not primarily due to time, and probably reflects the extent of under-immunosuppression.

Among biopsies with TCMR, the intensity declines with time in biopsies after the first 2 y posttransplant.[107] The declining mean intensity of TCMR activity, as well as the declining frequency of TCMR, probably reflects the adaptive changes in host T cell clones, for example, checkpoints.

Also in Figure 14B, EAMR is the first AMR phenotype, but FAMR becomes dominant after 1 y. Beyond 10 y posttransplant, both FAMR and LAMR are common, but EAMR becomes uncommon. We believe that the decline in new-onset AMR after 10 y indicates that a state of partial adaptive T-cell tolerance emerges over time, affecting the ability of T follicular helper T cells to initiate new pathogenic DSA responses.

Injury changes also accumulate with time posttransplant.[65,143] In Figure 14C, transcripts reflecting recent injury—AKI transcripts (IRRAT) and fibrillar collagen transcripts—are the highest early posttransplant and regress to lower levels in late biopsies. Molecular and histologic atrophy-fibrosis increases steadily with log time[66]: mast cell transcripts, IGTs, fibrosis classifier scores (ci>1_{Prob}), and histologic fibrosis.

Given the critical role of parenchymal injury in determining outcomes, we studied "injury-ness" in detail using the same approaches we used to define "rejection-ness,"[65,143] namely PCA and archetypal analysis. The details cannot be presented here due to lack of space but the key finding is that there is much information in the parenchyma that reveals diversity in the response to wounding and relationships to important issues such as donor aging.

Table 6 summarizes the mean molecular, clinical, and histologic features in the 6 rejection archetype groups.

Molecular Insights into Progression to Graft Failure After Biopsy

Figure 15A[108] compares survival after biopsy of kidneys with various rejection archetypes, using 1 random biopsy per patient. All rejection had impaired postbiopsy survival compared to no rejection, although onset of failures after EAMR biopsies was delayed by about 2 y as previously reported.[61]

We explore the relative importance of various rejection and injury parameters in predicting failure postbiopsy using random forests. We studied all biopsies[114] (Figure 15B), TCMR biopsies[108] (Figure 15C), and AMR biopsies[114] (Figure 15D). In all analyses, the dominant factors predicting survival were those related to parenchymal injury: IRRATs, a classifier for proteinuria that correlated with chronic injury, lowGFR_{Prob}, and the eGFR itself. Molecular rejection activity and histologic rejection activity was relatively unimportant.

Among biopsies with AMR, we compared the impact of DSA and AMR molecular activity to recent injury and atrophy-fibrosis (Figure 15E–H). Neither DSA positivity

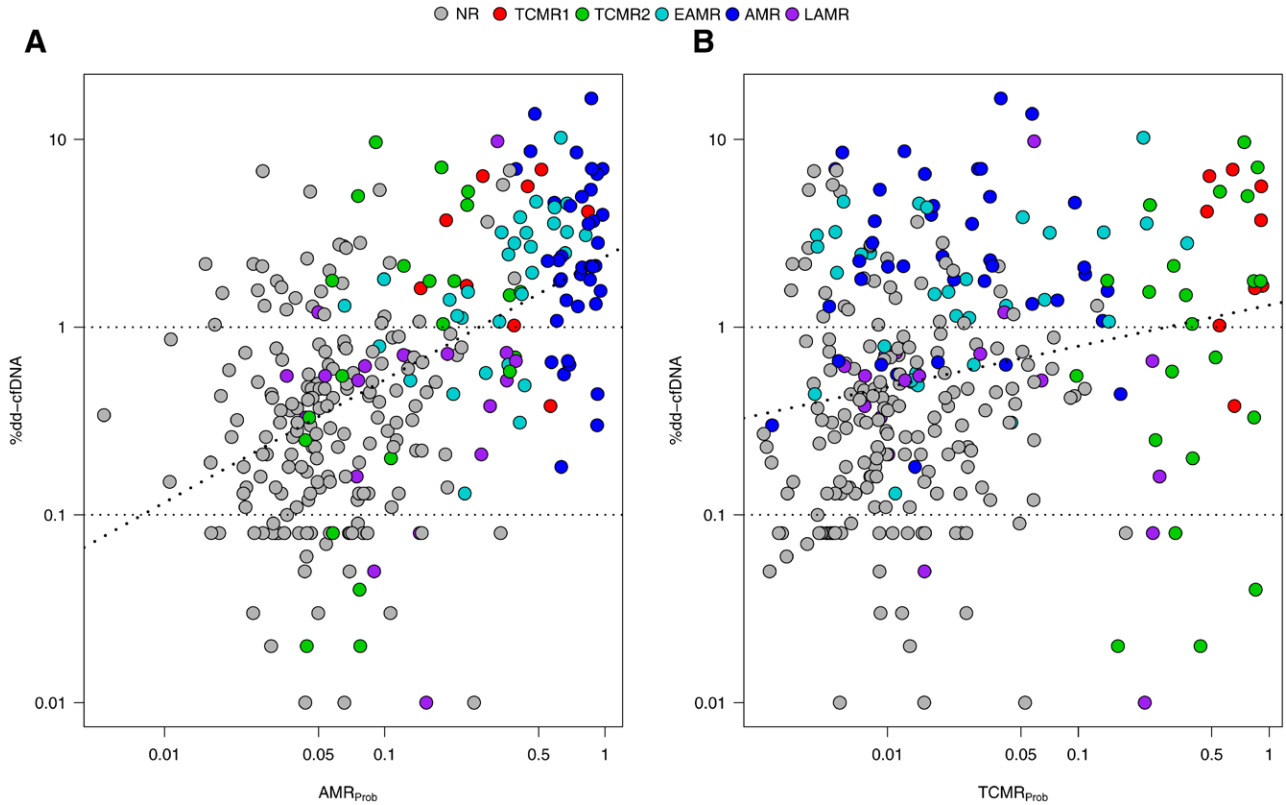

FIGURE 16. Relationships between %dd-cfDNA, molecular archetype groups, and the AMR_{Prob} and $TCMR_{Prob}$ classifier scores in N = 300 samples.[86] Dots represent biopsies and corresponding paired blood sample %dd-cfDNA results, colored by archetype cluster assignments. Regression lines (dashed) show the relationship between the (A) AMR_{Prob} and (B) $TCMR_{Prob}$ classifier scores and %dd-cfDNA. Spearman correlations with dd-cfDNA were stronger for AMR_{Prob} (0.52, P = 6E-22) than $TCMR_{Prob}$ (0.22, P = 9E-5). AMR, antibody-mediated rejection; dd-cfDNA, donor-derived cell-free DNA; EAMR, early-stage AMR; LAMR, late-stage AMR; NR, no rejection; TCMR, T cell–mediated rejection.

(Figure 15E) nor AMR_{Prob} activity (Figure 15F) impacted survival within the AMR cases. The only factors with major impact were the extent of recent injury (Figure 15G) and of atrophy-fibrosis (Figure 15H).

The dominance of parenchymal injury over disease activity in determining survival postbiopsy within kidney groups with AMR or TCMR recalls the classical analysis of survival postbiopsy within glomerulonephritis, which found that atrophy-fibrosis was the key determinant, not disease activity.[114]

In all comparisons of histology assessment versus molecular assessment, molecular parameters predict survival better than histologic parameters.[49,107,122,133,144] Histologic i-IFTA was significant in univariate analysis but dropped out in multivariate analysis when molecular injury and atrophy-fibrosis were included.[122]

Relating MMDx Biopsy Findings to dd-cfDNA Levels: The Trifecta Study

Dd-cfDNA has emerged as an objective parameter to follow the state of the transplanted kidney. The prospective Trifecta study[145] (ClinicalTrials.gov: NCT04239703) examined the relationships of centrally measured dd-cfDNA (by Natera, Inc.) and DSA (by One Lambda Inc.) to MMDx findings in indication biopsies. In the first analysis (300 biopsies from 289 recipients), we compared the dd-cfDNA drawn just before biopsy to the MMDx findings. The top 20 probe sets correlating with %dd-cfDNA were all previously annotated as selective for AMR activity, either natural killer (NK) cell-expressed (eg, GNLY, CCL4, TRDC, and S1PR5) or IFNG-inducible (eg, PLA1A, IDO1, CXCL11, and WARS). The dd-cfDNA correlated with the AMR_{Prob} score (Figure 16A) and less strongly with the $TCMR_{Prob}$ score (Figure 16B). dd-cfDNA was highest in AMR and mixed rejection, varied in TCMR, and was moderately elevated in recent injury (AKI). By multivariate random forests and logistic regression, dd-cfDNA levels correlated more strongly with molecular rejection than histologic rejection, similar to an earlier analysis.[4]

At the time of biopsy, plasma dd-cfDNA is a better predictor of molecular AMR in the biopsy than DSA, although the best predictions used both.[141] Dd-cfDNA quantity was more closely related to AMR activity than %dd-cfDNA as a fraction of total cfDNA, and the use of both quantity and percent in logistic regression improved the prediction of molecular rejection.[145] Importantly, we found that DSA-negative AMR was as strongly associated with high dd-cfDNA as DSA-positive AMR.[141]

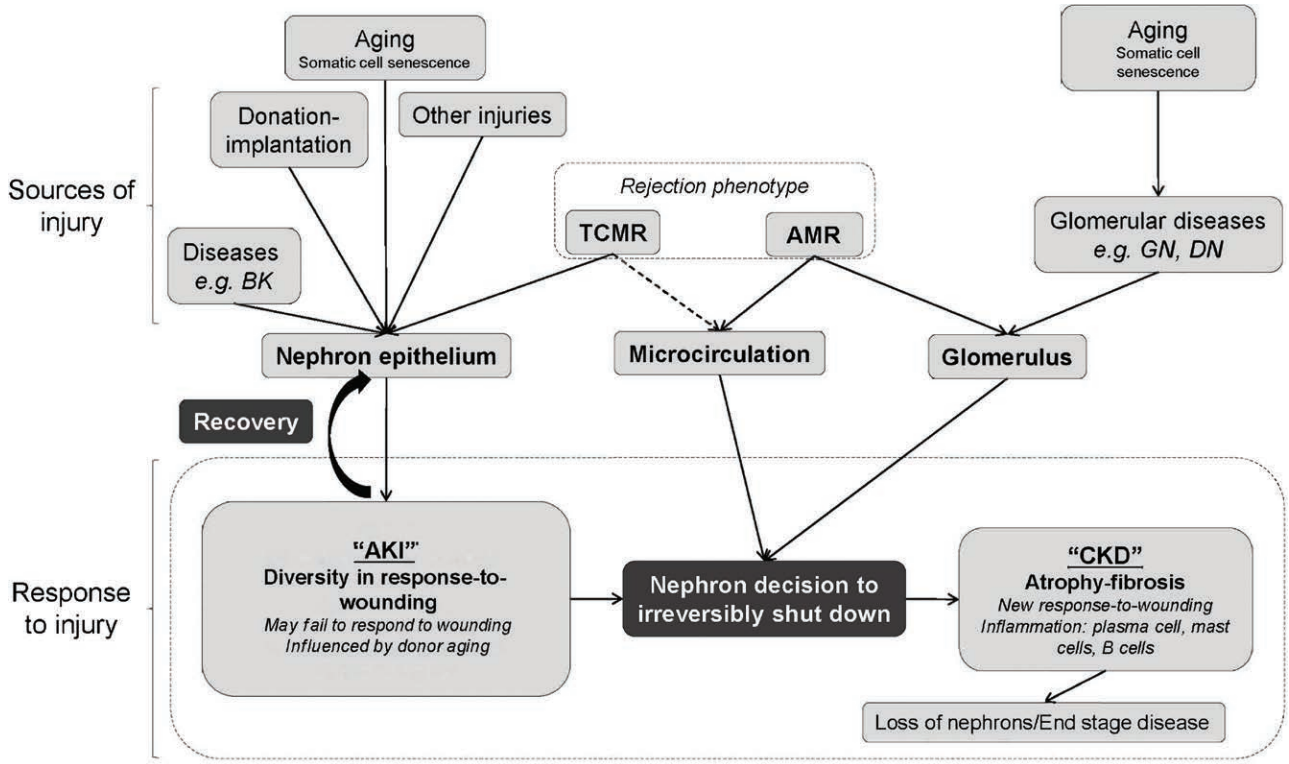

FIGURE 17. Schematic diagram representing the relationships between sources of injury and response to injury in kidney transplant biopsies based on injury analyses in MMDx.[143] Interplay between sources of injury, pre-existing limitations such as aging, and response to injury by the nephron. There are 2 routes to irreversible nephron shutdown, namely, direct epithelial injury and glomerulus injury with secondary nephron failure. Epithelial injury should trigger the response-to-wounding, which involves epithelium, matrix, and microcirculation, and evokes innate immunity. Failure to mount a response to wounding and adopting a "PC3"-related response (eg, PARD3) with minimal inflammation leads to failure to recover. Many sources of injury (separate from and including rejection) interact with the nephron epithelium, producing AKI. In this instance, the epithelium can be repaired and the organ can recover, or progress to nephron failure. Alternatively, aging and/or AMR can contribute to glomerular disease and AMR can additionally affect the microcirculation, affecting the glomerulus and again causing nephron shutdown, which eventually leads to CKD. If this occurs, a loss of nephrons and end-stage renal disease may occur. Different sources of injury may interact to cause many forms of injury, and injury itself predicts the graft survival while the rejection status does not. Thus, defining the heterogeneity within biopsy injury is an important part of clinical management. AKI, acute kidney injury; AMR, antibody-mediated rejection; CKD, chronic kidney disease; MMDx, Molecular Microscope Diagnostics System; TCMR, T cell–mediated rejection.

The striking correlation of dd-cfDNA with active AMR, even DSA-negative AMR, was established, and new studies are exploring the molecular basis of dd-cfDNA release. The emerging integrated view of injury and rejection on the kidney transplant is outlined in Figure 17.

Impact of MMDx and Relationship to Histology

There are several outputs from the MMDx project:

1. MMDx defines the genome-wide changes in renal tissue that accompany the major events in kidney transplant population reflecting the disease states—TCMR, AMR, AKI, and atrophy-fibrosis—and the relationship of these changes to time, dysfunction, and probability of failure. This information can be used to infer mechanisms and potential targets for intervention.
2. MMDx has been licensed as a diagnostic system to Thermo Fisher, which has established service laboratories in Portland and Prague. The prices for these services can be obtained by contacting these laboratories.
3. The findings in MMDx can guide development of other molecular platforms.
4. MMDx can be used to support clinical trials, as demonstrated in several recent studies.[146–151]
5. MMDx findings can be used to guide the evolution of the Banff diagnostic system.
6. MMDx can guide the development and calibration of noninvasive biomarkers in body fluids, as is occurring in the Trifecta studies for kidney, heart, and lung biopsies.

The advantages and limitations of the MMDx system and histology are compared in Table 7. Unresolved problems in MMDx include the ideal amount of tissue to be sent for MMDx. MMDx can assess even tiny samples reproducibly but the potential for sampling error rises as sample size decreases. MMDx has been built exclusively in clinical trials in which IRBs strictly limited the amounts of tissue available. Similar questions of sampling arise in all biopsy diagnostic systems, where the clinician must strike a balance between minimizing the size of the sample and the risk of sampling error. One possibility we are considering is to pool portions of 2 cores being taken for histology to reduce the reliance on 1 sample, avoiding medulla if possible.

How Can Molecular Biopsy Phenotyping Be Applied?

We believe that ideally histology and molecular biopsy phenotyping should be used, performed independently with a combined interpretation by the clinician and pathologist. However, the relationship of MMDx to histology in clinical practice will be determined by local preferences and health economics. MMDx can be used routinely along with histology for every biopsy, selectively for resolving ambiguous cases (when centers routinely save a portion of the biopsy in RNA*later*), or in some cases without histology. Currently MMDx has supported a number of clinical trials,[146–151] and can continue to be used as an endpoint when evaluating various interventions. MMDx is also a scientific reference—a repository for understanding the genome-wide changes that underlie the disease states in organ transplants. MMDx

TABLE 7.

Limitations and features of the MMDx compared to standard of care biopsy assessment by histology.

	Technology for transplant assessment	
	Histology-based biopsy assessment	**The MMDx**
Advantages	- Can be processed and interpreted quickly under some conditions. - Can assess primary diseases. - Can assess highly focal changes. - Can be supplemented by special stains, eg, polyoma virus SV40. - Processing locally can save shipping time.	- Automated measurements and fixed automated analysis algorithms are completely reproducible on the tissue provided. - Quick processing time, usually within 24 h of receipt of biopsy. - Provides scores as continuous numbers, preserving granularity. - Measures recent tissue injury (AKI) with gene sets/classifiers, which correlate with function and are important predictors of outcomes. - Designed to assess biopsies that are predominantly cortex, but can also estimate % cortical tissue in the sample, and can assess medulla (with caveats). - Derived entirely from data collected in registered clinical trials.
Limitations	- Subject to interobserver variation in determining step 1 features and applying step 2 guidelines to make a diagnosis. - Derived from clinical experience, not trials. - Subject to sampling error and heterogeneity in disease processes within the tissue. - Additional tests are required in Banff (C4d, DSA), which extend time to test result. - Results are usually given in categorical "grades," losing granularity (eg, 0, 1, 2, 3). - Cannot assess medulla tissue. Designed to read cortex, and should have glomeruli and arteries. - Assessment of recent injury (acute tubular injury) correlates poorly with function.	- Clinical trials dictated small sample size so subject to sampling error. Ideal sample size remains to be determined. - Must be shipped to a central lab. - May be affected by highly focal processes. - Cannot assess primary diseases. - The microarray does not measure virus transcripts. (However, the RNA already isolated from the biopsy can be rapidly tested for expression of virus mRNA using quantitative RT-PCR to measure virus activity in the biopsy.

AKI, acute kidney injury; DSA, donor-specific antibody; MMDx, Molecular Microscope Diagnostic System; mRNA, messenger RNA; RT-PCR, reverse transcription polymerase chain reaction.

findings can guide the development of other molecular biopsy assessment platforms measuring selected genes, for example, RTPCR, BHOT.[74,152,153] Genome-wide systems using RNA sequencing should also be developed for documenting details that cannot be explored in microarrays, for example, alternative mRNA splicing and alternative promoters.

Insights from molecular studies have opened many possibilities for new therapies in other fields of medicine, and using molecular insights to change management and improve outcomes remains the ultimate goal.

REFERENCES

1. Hariharan S, Israni AK, Danovitch G. Long-term survival after kidney transplantation. *N Engl J Med*. 2021;385:729–743.
2. Nankivell BJ, Kuypers DR. Diagnosis and prevention of chronic kidney allograft loss. *Lancet*. 2011;378:1428–1437.
3. Tait BD, Susal C, Gebel HM, et al. Consensus guidelines on the testing and clinical management issues associated with HLA and non-HLA antibodies in transplantation. *Transplantation*. 2013;95:19–47.
4. Gupta G, Moinuddin I, Kamal L, et al. Correlation of donor-derived cell-free DNA with histology and molecular diagnoses of kidney transplant biopsies. *Transplantation*. 2022;106:1061–1070.
5. Xiao H, Gao F, Pang Q, et al. Diagnostic Accuracy of donor-derived cell-free DNA in renal-allograft rejection: a meta-analysis. *Transplantation*. 2021;105:1303–1310.
6. Filippone EJ, Farber JL. The monitoring of donor-derived cell-free DNA in kidney transplantation. *Transplantation*. 2021;105:509–516.
7. Halloran PF, Famulski K, Reeve J. The molecular phenotypes of rejection in kidney transplant biopsies. *Curr Opin Organ Transplant*. 2015;20:359–367.
8. Halloran PF, Reeve JP, Pereira AB, et al. Antibody-mediated rejection, T cell-mediated rejection, and the injury-repair response: new insights from the Genome Canada studies of kidney transplant biopsies. *Kidney Int*. 2014;85:258–264.
9. Reeve J, Halloran PF, Kaplan B. Common errors in the implementation and interpretation of microarray studies. *Transplantation*. 2015;99:470–475.
10. Halloran PF, Famulski KS, Reeve J. Molecular assessment of disease states in kidney transplant biopsy samples. *Nat Rev Nephrol*. 2016;12:534–548.
11. Halloran PF, Venner JM, Madill-Thomsen KS, et al. Review: the transcripts associated with organ allograft rejection. *Am J Transplant*. 2018;18:785–795.
12. Halloran PF, Madill-Thomsen KS. The molecular microscope diagnostic system: assessment of rejection and injury in heart transplant biopsies. *Transplantation*. 2023;107:27–44.
13. Halloran P, Festenstein H. Inhibition of cell-dependent cytotoxicity as an assay for mouse alloantibody. *Nature*. 1974;250:52–54.
14. Halloran P, Schirrmacher V, Festenstein H. A new sensitive assay for antibody against cell surface antigens based on inhibition of cell-dependent antibody-mediated cytotoxicity. I. Specificity and sensitivity. *J Exp Med*. 1974;140:1348–1363.
15. Wadgymar A, Urmson J, Baumal R, et al. Changes in Ia expression in mouse kidney during acute graft-vs-host disease. *J Immunol*. 1984;132:1826–1832.
16. Sinclair GD, Wadgymar A, Halloran PF, et al. Graft-vs-host reactions induce H-2 class-Ii gene-transcription in host kidney-cells. *Immunogenetics*. 1984;20:503–511.
17. Milton AD, Spencer SC, Fabre JW. Detailed analysis and demonstration of differences in the kinetics of induction of class I and class II major histocompatibility complex antigens in rejecting cardiac and kidney allografts in the rat. *Transplantation*. 1986;41:499–508.
18. Hall BM, Bishop GA, Duggin GG, et al. Increased expression of HLA-DR antigens on renal tubular cells in renal transplants: relevance to the rejection response. *Lancet*. 1984;2:247–251.
19. Halloran PF, Afrouzian M, Ramassar V, et al. Interferon-gamma acts directly on rejecting renal allografts to prevent graft necrosis. *Am J Pathol*. 2001;158:215–226.
20. Afrouzian M, Ramassar V, Urmson J, et al. Transcription factor IRF-1 in kidney transplants mediates resistance to graft necrosis during rejection. *J Am Soc Nephrol*. 2002;13:1199–1209.
21. Halloran PF, Miller LW, Urmson J, et al. IFN-gamma alters the pathology of graft rejection: protection from early necrosis. *J Immunol*. 2001;166:7072–7081.
22. Goes N, Urmson J, Vincent D, et al. Induction of major histocompatibility complex and inflammatory cytokines after ischemic injury to the kidney: lessons from the interferon-γ gene knockout mice. *Transplant Proc*. 1995;27:771–773.
23. Shoskes DA, Parfrey NA, Halloran PF. Increased major histocompatibility complex antigen expression in unilateral ischemic acute tubular necrosis in the mouse. *Transplantation*. 1990;49:201–207.
24. Shoskes DA, Halloran PF. Ischemic injury induces altered MHC gene expression in kidney by an interferon-gamma-dependent pathway. *Transplant Proc*. 1991;23(1 Pt 1):599–601.
25. Wiskocil R, Weiss A, Imboden J, et al. Activation of a human T cell line: a two-stimulus requirement in the pre-translational events involved in the co-ordinate expression of interleukin-2 and gamma-interferon genes. *J Immunol*. 1985;134:1599–1603.
26. Ooi BS, Jao W, First MR, et al. Acute interstitial nephritis. A clinical and pathologic study based on renal biopsies. *Am J Med*. 1975;59:614–628.
27. Sibley RK, Rynasiewicz J, Ferguson RM, et al. Morphology of cyclosporine nephrotoxicity and acute rejection in patients immunosuppressed with cyclosporine and prednisone. *Surgery*. 1983;94:225–234.
28. Verani RR, Flechner SM, Van Buren CT, et al. Acute cellular rejection or cyclosporine A nephrotoxicity? A review of transplant renal biopsies. *Am J Kidney Dis*. 1984;4:185–191.
29. Beschorner WE, Burdick JF, Williams GM, et al. The presence of Leu-7 reactive lymphocytes in renal-allografts undergoing acute rejection. *Transplant Proc*. 1985;17:618–622.
30. Solez K, Axelsen RA, Benediktsson H, et al. International standardization of criteria for the histologic diagnosis of renal allograft rejection: the Banff working classification of kidney transplant pathology. *Kidney Int*. 1993;44:411–422.
31. Jabs WJ, Sedlmeyer A, Ramassar V, et al. Heterogeneity in the evolution and mechanisms of the lesions of kidney allograft rejection in mice. *Am J Transplant*. 2003;3:1501–1509.
32. Famulski KS, Einecke G, Reeve J, et al. Changes in the transcriptome in allograft rejection: IFN-γ induced transcripts in mouse kidney allografts. *Am J Transplant*. 2006;6:1342–1354.
33. Einecke G, Fairhead T, Hidalgo LG, et al. Tubulitis and epithelial cell alterations in mouse kidney transplant rejection are independent of CD103, perforin or granzymes A/B. *Am J Transplant*. 2006;6:2109–2120.
34. Lanier LL. NK cell receptors. *Ann Rev Immunol*. 1998;16:359–393.
35. Coenon L, Villalba M. From CD16a biology to antibody-dependent cell-mediated cytotoxicity improvement. *Front Immunol*. 2022;13:913215.
36. Halloran PF, Wadgymar A, Ritchie S, et al. The significance of the anti-class I antibody response. I. Clinical and pathologic features of anti-class I-mediated rejection. *Transplantation*. 1990;49:85–91.
37. Bohmig GA, Halloran PF, Feucht HE. On a long and winding road—alloantibodies in organ transplantation. *Transplantation*. In press.
38. Feucht HE, Felber E, Gokel MJ, et al. Vascular deposition of complement-split products in kidney allografts with cell-mediated rejection. *Clin Exp Immunol*. 1991;86:464–470.
39. Feucht HE. Complement C4d in graft capillaries—the missing link in the recognition of humoral alloreactivity. *Am J Transplant*. 2003;3:646–652.
40. Racusen LC, Colvin RB, Solez K, et al. Antibody-mediated rejection criteria—an addition to the Banff 97 classification of renal allograft rejection. *Am J Transplant*. 2003;3:708–714.
41. Sis B, Jhangri GS, Bunnag S, et al. Endothelial gene expression in kidney transplants with alloantibody indicates antibody-mediated damage despite lack of C4d staining. *Am J Transplant*. 2009;9:2312–2323.
42. Halloran PF, Madill-Thomsen KS, Pon S, et al; INTERCOMEX Investigators. Molecular diagnosis of ABMR with or without donor-specific antibody in kidney transplant biopsies: differences in timing and intensity but similar mechanisms and outcomes. *Am J Transplant*. 2022;22:1976–1991.
43. Hidalgo LG, Einecke G, Allanach K, et al. The transcriptome of human cytotoxic T cells: measuring the burden of CTL-associated transcripts in human kidney transplants. *Am J Transplant*. 2008;8:637–646.
44. Hidalgo LG, Sis B, Sellares J, et al. NK cell transcripts and NK cells in kidney biopsies from patients with donor-specific antibodies: evidence for NK cell involvement in antibody-mediated rejection. *Am J Transplant*. 2010;10:1812–1822.

45. Hidalgo LG, Sellares J, Sis B, et al. Interpreting NK cell transcripts versus T cell transcripts in renal transplant biopsies. *Am J Transplant*. 2012;12:1180–1191.
46. Halloran PF, Potena L, Van Huyen JD, et al. Building a tissue-based molecular diagnostic system in heart transplant rejection: the heart Molecular Microscope Diagnostic (MMDx) System. *J Heart Lung Transplant*. 2017;36:1192–1200.
47. Halloran PF, Venner JM, Famulski KS. Comprehensive analysis of transcript changes associated with allograft rejection: combining universal and selective features. *Am J Transplant*. 2017;17:1754–1769.
48. Famulski KS, de Freitas DG, Kreepala C, et al. Molecular phenotypes of acute kidney injury in kidney transplants. *J Am Soc Nephrol*. 2012;23:948–958.
49. Famulski KS, Reeve J, de Freitas DG, et al. Kidney transplants with progressing chronic diseases express high levels of acute kidney injury transcripts. *Am J Transplant*. 2013;13:634–644.
50. Famulski KS, Broderick G, Einecke G, et al. Transcriptome analysis reveals heterogeneity in the injury response of kidney transplants. *Am J Transplant*. 2007;7:2483–2495.
51. Einecke G, Reeve J, Mengel M, et al. Expression of B cell and immunoglobulin transcripts is a feature of inflammation in late allografts. *Am J Transplant*. 2008;8:1434–1443.
52. Einecke G, Melk A, Ramassar V, et al. Expression of CTL associated transcripts precedes the development of tubulitis in T-cell mediated kidney graft rejection. *Am J Transplant*. 2005;5:1827–1836.
53. Famulski KS, Sis B, Billesberger L, et al. Interferon-gamma and donor MHC class I control alternative macrophage activation and activin expression in rejecting kidney allografts: a shift in the Th1-Th2 paradigm. *Am J Transplant*. 2008;8:547–556.
54. Famulski KS, Einecke G, Sis B, et al. Defining the canonical form of T-cell-mediated rejection in human kidney transplants. *Am J Transplant*. 2010;10:810–820.
55. Hidalgo LG, Einecke G, Allanach K, et al. The transcriptome of human cytotoxic T cells: similarities and disparities among allostimulated CD4(+) CTL, CD8(+) CTL and NK cells. *Am J Transplant*. 2008;8:627–636.
56. Einecke G, Kayser D, Vanslambrouck JM, et al. Loss of solute carriers in T cell-mediated rejection in mouse and human kidneys: an active epithelial injury-repair response. *Am J Transplant*. 2010;10:2241–2251.
57. Einecke G, Broderick G, Sis B, et al. Early loss of renal transcripts in kidney allografts: relationship to the development of histologic lesions and alloimmune effector mechanisms. *Am J Transplant*. 2007;7:1121–1130.
58. Mengel M, Chang J, Kayser D, et al. The molecular phenotype of six-week protocol biopsies from human renal allografts: reflections of prior injury but not future course. *Am J Transplant*. 2011;11:708–718.
59. Reeve J, Bohmig GA, Eskandary F, et al; INTERCOMEX MMDx-Kidney Study Group. Generating automated kidney transplant biopsy reports combining molecular measurements with ensembles of machine learning classifiers. *Am J Transplant*. 2019;19:2719–2731.
60. Reeve J, Sellares J, Mengel M, et al. Molecular diagnosis of T cell-mediated rejection in human kidney transplant biopsies. *Am J Transplant*. 2013;13:645–655.
61. Reeve J, Bohmig GA, Eskandary F, et al. Assessing rejection-related disease in kidney transplant biopsies based on archetypal analysis of molecular phenotypes. *JCI Insight*. 2017;2:e94197.
62. Sellares J, Reeve J, Loupy A, et al. Molecular diagnosis of antibody-mediated rejection in human kidney transplants. *Am J Transplant*. 2013;13:971–983.
63. Madill-Thomsen KS, Bohmig GA, Bromberg J, et al; INTERCOMEX Investigators. Donor-specific antibody is associated with increased expression of rejection transcripts in renal transplant biopsies classified as no rejection. *J Am Soc Nephrol*. 2021;32:2743–2758.
64. Reeve J, Einecke G, Mengel M, et al. Diagnosing rejection in renal transplants: a comparison of molecular- and histopathology-based approaches. *Am J Transplant*. 2009;9:1802–1810.
65. Halloran PF, Bohmig GA, Bromberg JS, et al; INTERCOMEX investigators. Discovering novel injury features in kidney transplant biopsies associated with TCMR and donor aging. *Am J Transplant*. 2021;21:1725–1739.
66. Venner JM, Famulski KS, Reeve J, et al. Relationships among injury, fibrosis, and time in human kidney transplants. *JCI Insight*. 2016;1:e85323.
67. Allison DB, Cui X, Page GP, et al. Microarray data analysis: from disarray to consolidation and consensus. *Nat Rev Genet*. 2006;7:55–65.
68. Dupuy A, Simon RM. Critical review of published microarray studies for cancer outcome and guidelines on statistical analysis and reporting. *J Natl Cancer Inst*. 2007;99:147–157.
69. Uhlen M, Fagerberg L, Hallstrom BM, et al. Proteomics. Tissue-based map of the human proteome. *Science*. 2015;347:1260419.
70. Malone AF, Humphreys BD. Single-cell transcriptomics and solid organ transplantation. *Transplantation*. 2019;103:1776–1782.
71. Peereboom ETM, Matern BM, Spierings E, et al. The value of single-cell technologies in solid organ transplantation studies. *Transplantation*. 2022;106:2325–2337.
72. Madill-Thomsen KS, Wiggins RC, Eskandary F, et al. The effect of cortex/medulla proportions on molecular diagnoses in kidney transplant biopsies: rejection and injury can be assessed in medulla. *Am J Transplant*. 2017;17:2117–2128.
73. Archer KJ, Mas VR, O'Brien TR, et al. Quality assessment of microarray data in a multicenter study. *Diagn Mol Pathol*. 2009;18:34–43.
74. Rosales IA, Mahowald GK, Tomaszewski K, et al. Banff human organ transplant transcripts correlate with renal allograft pathology and outcome: importance of capillaritis and subpathologic rejection. *J Am Soc Nephrol*. 2022;33:2306–2319.
75. Affymetrix. GeneChip® PrimeView™ Human Gene Expression Array data sheet:1–4. Available at http://www.affymetrix.com/support/technical/datasheets/primeview_array_cartridge_datasheet.pdf. Accessed October 6, 2022.
76. Topol E. *Deep Medicine: How Artificial Intelligence Can Make Healthcare Human Again*. 1st ed. Basic Books; 2019.
77. Labriffe M, Woillard JB, Gwinner W, et al. Machine learning-supported interpretation of kidney graft elementary lesions in combination with clinical data. *Am J Transplant*. 2022;22:2821–2833.
78. Mueller TF, Einecke G, Reeve J, et al. Microarray analysis of rejection in human kidney transplants using pathogenesis-based transcript sets. *Am J Transplant*. 2007;7:2712–2722.
79. Venner JM, Famulski KS, Badr D, et al. Molecular landscape of T cell-mediated rejection in human kidney transplants: prominence of CTLA4 and PD ligands. *Am J Transplant*. 2014;14:2565–2576.
80. Venner JM, Hidalgo LG, Famulski KS, et al. The molecular landscape of antibody-mediated kidney transplant rejection: evidence for NK involvement through CD16a Fc receptors. *Am J Transplant*. 2015;15:1336–1348.
81. Ioannidis JP. How to make more published research true. *PLoS Med*. 2014;11:e1001747.
82. Walch JM, Zeng Q, Li Q, et al. Cognate antigen directs CD8+ T cell migration to vascularized transplants. *J Clin Invest*. 2013;123:2663–2671.
83. Stefanidakis M, Newton G, Lee WY, et al. Endothelial CD47 interaction with SIRPgamma is required for human T-cell transendothelial migration under shear flow conditions in vitro. *Blood*. 2008;112:1280–1289.
84. Tedla FM, Sanchez Russo L, Menon MC. Outfoxing Rejection: urinary FOXP3 mRNA, TCMR, and the Fate of Allografts. *Transplantation*. 2021;105:1662–1663.
85. Bunnag S, Allanach K, Jhangri GS, et al. FOXP3 expression in human kidney transplant biopsies is associated with rejection and time post transplant but not with favorable outcomes. *Am J Transplant*. 2008;8:1423–1433.
86. Halloran PF, Reeve J, Madill-Thomsen KS, et al; Trifecta Investigators. The Trifecta study: comparing plasma levels of donor-derived cell-free DNA with the molecular phenotype of kidney transplant biopsies. *J Am Soc Nephrol*. 2022;33:387–400.
87. Aubert O, Kamar N, Vernerey D, et al. Long term outcomes of transplantation using kidneys from expanded criteria donors: prospective, population based cohort study. *BMJ*. 2015;351:h3557.
88. Charreau B. Cellular and molecular crosstalk of graft endothelial cells during AMR: effector Functions and mechanisms. *Transplantation*. 2021;105:e156–e167.
89. Halloran PF, Merino Lopez M, Barreto Pereira A. Identifying subphenotypes of antibody-mediated rejection in kidney transplants. *Am J Transplant*. 2016;16:908–920.
90. Parkes MD, Halloran PF, Hidalgo LG. Direct evidence for CD16a-mediated NK cell stimulation in antibody-mediated kidney transplant rejection. *Transplantation*. 2017;101:e102–e111.
91. Parkes M, Halloran P, Hidalgo L. CD16a-Activated NK Cells in ABMR Are Highly Similar to CD3-Activated Effector T Cells in TCMR. *Am J Transplant*. 2017;17:222–222.
92. Diebolder CA, Beurskens FJ, de Jong RN, et al. Complement is activated by IgG hexamers assembled at the cell surface. *Science*. 2014;343:1260–1263.

93. Zhang Y, Boesen CC, Radaev S, et al. Crystal structure of the extracellular domain of a human Fc gamma RIII. *Immunity*. 2000;13:387–395.
94. Halloran PF. Immunosuppressive drugs for kidney transplantation. *N Engl J Med*. 2004;351:2715–2729.
95. Koenig A, Mezaache S, Callemeyn J, et al. Missing self-induced activation of NK cells combines with non-complement-fixing donor-specific antibodies to accelerate kidney transplant loss in chronic antibody-mediated rejection. *J Am Soc Nephrol*. 2021;32:479–494.
96. Pahl JHW, Koch J, Gotz JJ, et al. CD16A Activation of NK cells promotes NK cell proliferation and memory-like cytotoxicity against cancer cells. *Cancer Immunol Res*. 2018;6:517–527.
97. Lanier LL, Corliss B, Wu J, et al. Association of DAP12 with activating CD94/NKG2C NK cell receptors. *Immunity*. 1998;8:693–701.
98. Lanier LL. NK cell receptors. *Annu Rev Immunol*. 1998;16:359–393.
99. Parham P, Guethlein LA. Genetics of natural killer cells in human health, disease, and survival. *Annu Rev Immunol*. 2018;36:519–548.
100. Bournazos S, Wang TT, Dahan R, et al. Signaling by antibodies: recent progress. *Annu Rev Immunol*. 2017;35:285–311.
101. Raghavan M, Bjorkman PJ. Fc receptors and their interactions with immunoglobulins. *Annu Rev Cell Dev Biol*. 1996;12:181–220.
102. Radaev S, Sun PD. Structure and function of natural killer cell surface receptors. *Annu Rev Biophys Biomol Struct*. 2003;32:93–114.
103. Callemeyn J, Lamarthee B, Koenig A, et al. Allorecognition and the spectrum of kidney transplant rejection. *Kidney Int*. 2022;101:692–710.
104. Halloran PF, Pereira AB, Chang J, et al. Potential impact of microarray diagnosis of T cell-mediated rejection in kidney transplants: the INTERCOM study. *Am J Transplant*. 2013;13:2352–2363.
105. Halloran PF, Pereira AB, Chang J, et al. Microarray diagnosis of antibody-mediated rejection in kidney transplant biopsies: an international prospective study (INTERCOM). *Am J Transplant*. 2013;13:2865–2874.
106. Einecke G, Sis B, Reeve J, et al. Antibody-mediated microcirculation injury is the major cause of late kidney transplant failure. *Am J Transplant*. 2009;9:2520–2531.
107. Halloran PF, Chang J, Famulski K, et al. Disappearance of T cell-mediated rejection despite continued antibody-mediated rejection in late kidney transplant recipients. *J Am Soc Nephrol*. 2015;26:1711–1720.
108. Madill-Thomsen KS, Bohmig GA, Bromberg J, et al. Relating molecular T cell-mediated rejection activity in kidney transplant biopsies to time and to histologic tubulitis and atrophy-fibrosis. *Transplantation*. [Epub ahead of print. 2022]. doi:10.1097/TP.0000000000004396
109. Nankivell BJ, P'Ng CH, O'Connell PJ, et al. Calcineurin inhibitor nephrotoxicity through the lens of longitudinal histology: comparison of cyclosporine and tacrolimus eras. *Transplantation*. 2016;100:1723–1731.
110. Aubert O, Loupy A, Hidalgo L, et al. Antibody-mediated rejection due to preexisting versus de novo donor-specific antibodies in kidney allograft recipients. *J Am Soc Nephrol*. 2017;28:1912–1923.
111. Loupy A, Lefaucheur C, Vernerey D, et al. Molecular microscope strategy to improve risk stratification in early antibody-mediated kidney allograft rejection. *J Am Soc Nephrol*. 2014;25:2267–2277.
112. Jeannet M, Pinn VW, Flax MH, et al. Humoral antibodies in renal allotransplantation in man. *N Engl J Med*. 1970;282:111–117.
113. Wu K, Budde K, Schmidt D, et al. The relationship of the severity and category of acute rejection with intimal arteritis defined in Banff classification to clinical outcomes. *Transplantation*. 2015;99:e105–e114.
114. Einecke G, Reeve J, Gupta G, et al; INTERCOMEX investigators. Factors associated with kidney graft survival in pure antibody-mediated rejection at the time of indication biopsy: importance of parenchymal injury but not disease activity. *Am J Transplant*. 2021;21:1391–1401.
115. Salazar IDR, Lopez MM, Chang J, et al. Reassessing the significance of v-lesions in kidney transplant biopsies. *J Am Soc Nephrol*. 2015;26:3190–3198.
116. Madill-Thomsen K, Perkowska-Ptasinska A, Bohmig GA, et al; MMDx-Kidney Study Group. Discrepancy analysis comparing molecular and histology diagnoses in kidney transplant biopsies. *Am J Transplant*. 2020;20:1341–1350.
117. Lefaucheur C, Loupy A, Vernerey D, et al. Antibody-mediated vascular rejection of kidney allografts: a population-based study. *Lancet*. 2013;381:313–319.
118. Nankivell BJ, Shingde M, Keung KL, et al. The causes, significance and consequences of inflammatory fibrosis in kidney transplantation: The Banff i-IFTA lesion. *Am J Transplant*. 2018;18:364–376.
119. Mengel M, Reeve J, Bunnag S, et al. Scoring total inflammation is superior to the current Banff inflammation score in predicting outcome and the degree of molecular disturbance in renal allografts. *Am J Transplant*. 2009;9:1859–1867.
120. Loupy A, Haas M, Solez K, et al. The Banff 2015 kidney meeting report: current challenges in rejection classification and prospects for adopting molecular pathology. *Am J Transplant*. 2017;17:28–41.
121. Halloran PF, Chang J, Famulski KS. Inflammation in scarred areas (i-IFTA) is a reflection of parenchymal injury (response to wounding) not T cell-mediated rejection. *Am J Transplant*. 2018;18:328–328.
122. Halloran PF, Matas A, Kasiske BL, et al. Molecular phenotype of kidney transplant indication biopsies with inflammation in scarred areas. *Am J Transplant*. 2019;19:1356–1370.
123. Helgeson ES, Mannon R, Grande J, et al. i-IFTA and chronic active T cell-mediated rejection: a tale of 2 (DeKAF) cohorts. *Am J Transplant*. 2021;21:1866–1877.
124. Haas M, Loupy A, Lefaucheur C, et al. The Banff 2017 Kidney Meeting Report: revised diagnostic criteria for chronic active T cell-mediated rejection, antibody-mediated rejection, and prospects for integrative endpoints for next-generation clinical trials. *Am J Transplant*. 2018;18:293–307.
125. Halloran PF, Madill-Thomsen KS, Bohmig GA, et al; INTERCOMEX Investigators. A 2-fold approach to polyoma virus (BK) nephropathy in kidney transplants: distinguishing direct virus effects from cognate T cell-mediated Inflammation. *Transplantation*. 2021;105:2374–2384.
126. Halloran PF, Gupta G, Reeve J; The INTERCOMEX Investigators. The complexity of T cell-mediated rejection scenarios: identifying BK in biopsies with TCMR. *Am J Transplant*. 2019;19:546–546.
127. Sellares J, De Freitas D, Mengel M, et al. Understanding the causes of kidney transplant failure: the dominant role of antibody-mediated rejection and non-adherence. *Am J Transplant*. 2012;12:388–399.
128. Higdon LE, Tan JC, Maltzman JS. Infection, rejection, and the connection. *Transplantation*. 2023;107:584–595.
129. Nankivell BJ, Agrawal N, Sharma A, et al. The clinical and pathological significance of borderline T cell-mediated rejection. *Am J Transplant*. 2019;19:1452–1463.
130. Vitalone MJ, O'Connell PJ, Wavamunno M, et al. Transcriptome changes of chronic tubulointerstitial damage in early kidney transplantation. *Transplantation*. 2010;89:537–547.
131. O'Connell PJ, Zhang W, Menon MC, et al. Biopsy transcriptome expression profiling to identify kidney transplants at risk of chronic injury: a multicentre, prospective study. *Lancet*. 2016;388:983–993.
132. Han WK, Bailly V, Abichandani R, et al. Kidney injury molecule-1 (KIM-1): a novel biomarker for human renal proximal tubule injury. *Kidney Int*. 2002;62:237–244.
133. Einecke G, Mengel M, Hidalgo LG, et al. The early course of renal allograft rejection: defining the time when rejection begins. *Am J Transplant*. 2009;9:483–493.
134. Dvorak HF. Tumors: wounds that do not heal-redux. *Cancer Immunol Res*. 2015;3:1–11.
135. Mengel M, Reeve J, Bunnag S, et al. Molecular correlates of scarring in kidney transplants: the emergence of mast cell transcripts. *Am J Transplant*. 2009;9:169–178.
136. Kreepala C, Famulski KS, Halloran PF. Fundamental concepts regarding graft injury and regeneration: tissue injury, tissue quality and recipient factors. In: Kirk AD, Knechtle SJ, Larsen CP, Madsen JC, Pearson TC, Webber SA, eds. *Textbook of Organ Transplantation*. 1st ed. John Wiley & Sons, Ltd; 2014:99–118.
137. Halloran PF, Famulski KS, Chang J. A probabilistic approach to histologic diagnosis of antibody-mediated rejection in kidney transplant biopsies. *Am J Transplant*. 2017;17:129–139.
138. Einecke G, Reeve J, Halloran PF. A molecular biopsy test based on arteriolar under-hyalinosis reflects increased probability of rejection related to under-immunosuppression. *Am J Transplant*. 2018;18:821–831.
139. Einecke G, Reeve J, Halloran PF. Hyalinosis lesions in renal transplant biopsies: time-dependent complexity of interpretation. *Am J Transplant*. 2017;17:1346–1357.
140. Senev A, Callemeyn J, Lerut E, et al. Histological picture of ABMR without HLA-DSA: temporal dynamics of effector mechanisms are relevant in disease reclassification. *Am J Transplant*. 2019;19:954–955.
141. Halloran PF, Reeve J, Madill-Thomsen KS, et al; the Trifecta Investigators. Antibody-mediated rejection without detectable donor-specific antibody releases donor-derived cell-free DNA: results from the Trifecta study. *Transplantation*. 2023;107:709–719.

142. von Andrian UH, MacKay CR. Advances in immunology: T-cell function and migration - Two sides of the same coin. *N Eng J Med*. 2000;343:1020–1033.
143. Halloran PF, Böhmig GA, Bromberg J, et al. Archetypal analysis of injury in kidney transplant biopsies identifies two classes of early AKI. *Front Med*. 2022;9:817324.
144. Einecke G, Reeve J, Sis B, et al. A molecular classifier for predicting future graft loss in late kidney transplant biopsies. *J Clin Invest*. 2010;120:1862–1872.
145. Halloran PF, Reeve J, Madill-Thomsen KS, et al; Trifecta Investigators*. Combining donor-derived cell-free DNA fraction and quantity to detect kidney transplant rejection using molecular diagnoses and histology as confirmation. *Transplantation*. 2022;106:2435–2442.
146. Kumar D, Raynaud M, Chang J, et al. Impact of belatacept conversion on renal function, histology, and gene expression in kidney transplant patients with chronic active antibody-mediated rejection. *Transplantation*. 2021;105:660–667.
147. Kumar D, Yakubu I, Safavi F, et al. Lack of response to tocilizumab in kidney transplant recipients with chronic ABMR. *Kidney360*. 2020;1:663–670.
148. Gupta G, Raynaud M, Kumar D, et al. Impact of belatacept conversion on kidney transplant function, histology, and gene expression—a single-center study. *Transpl Int*. 2020;33:1458–1471.
149. Doberer K, Duerr M, Halloran PF, et al. A randomized trial of anti-interleukin-6 antibody clazakizumab in late antibody-mediated kidney transplant rejection. *J Am Soc Nephrol*. 2020;32:708–722.
150. Doberer K, Klager J, Gualdoni GA, et al. CD38 antibody daratumumab for the treatment of chronic active antibody-mediated kidney allograft rejection. *Transplantation*. 2021;105:451–457.
151. Eskandary F, Regel H, Baumann L, et al. A randomized, placebo-controlled trial of bortezomib in late antibody-mediated kidney transplant rejection: the BORTEJECT Study. *J Am Soc Nephrol*. 2017;29:591–605.
152. Smith RN. In-silico performance, validation, and modeling of the Nanostring Banff Human Organ transplant gene panel using archival data from human kidney transplants. *BMC Med Genomics*. 2021;14:86.
153. Mengel M, Loupy A, Haas M, et al. Banff 2019 Meeting Report: molecular diagnostics in solid organ transplantation-Consensus for the Banff Human Organ Transplant (B-HOT) gene panel and open source multicenter validation. *Am J Transplant*. 2020;20:2305–2317.
154. Fusfeld L, Menon S, Gupta G, et al. US payer budget impact of a microarray assay with machine learning to evaluate kidney transplant rejection in for-cause biopsies. *J Med Econ*. 2022;25:515–523.